PLOS ONE

Area and volumetric density estimation in processed full-field digital mammograms for risk assessment of breast cancer

--Manuscript Draft--

Manuscript Number:	PONE-D-14-25713R1
Article Type:	Research Article
Full Title:	Area and volumetric density estimation in processed full-field digital mammograms for risk assessment of breast cancer
Short Title:	Density estimation in processed full-field digital mammograms
Corresponding Author:	Abbas Cheddad Karolinska Institutet Stockholm, SWEDEN
Keywords:	Breast cancer risk; mammographic density; Features; ZNF365; Volpara; FFDM.
Abstract:	Introduction: Mammographic density, the white radiolucent part of a mammogram, is a marker of breast cancer risk and mammographic sensitivity. There are several means of measuring mammographic density, among which are area-based and volumetric-based approaches. Current volumetric methods use only unprocessed, raw, mammograms, which is a problematic restriction since such raw mammograms are normally not stored. We describe fully automated methods for measuring both area and volumetric mammographic density from processed images. Methods: The data set used in this study comprises raw and processed images of the same view from 1462 women. We developed two algorithms for processed images, an automated area-based approach (CASAM-Area) and a volumetric-based approach (CASAM-Vol). The latter method was based on training a random forest prediction model with image statistical features as predictors, against a volumetric measure, Volpara®, for corresponding raw images. We contrast the three methods, CASAM-Area, CASAM-Vol and Volpara directly and in terms of association with breast cancer risk and a known genetic variant for mammographic density and breast cancer, rs10995190 in the gene ZNF365. Associations with breast cancer risk were evaluated using images from 47 breast cancer cases and 1011 control subjects. The genetic association analysis was based on 1011 control subjects. Results: All three measures of mammographic density were associated with breast cancer risk and rs10995190 ($p < 0.025$ for breast cancer risk and $p < 1\times10\text{-}6$ for rs10995190). After adjusting for one of the measures there remained little or no evidence of residual association with the remaining density measures ($p > 0.10$ for risk, $p > 0.03$ for rs10995190). Conclusions: Our results show that it is possible to obtain reliable automated measures of volumetric and area mammographic density from processed digital images. Area and volumetric measures of density on processed digital images performed similar in terms of risk and genetic association.
Order of Authors:	Abbas Cheddad
	Kamila Czene
	Mikael Eriksson
	Jingmei Li
	Douglas Easton
	Per Hall
	Keith Humphreys
Response to Reviewers:	Respond to Reviewers is uploaded as a separate file.
Additional Information:	

Question	Response
Financial Disclosure Please describe all sources of funding that have supported your work. A complete funding statement should do the following: Include **grant numbers and the URLs** of any funder's website. Use the full name, not acronyms, of funding institutions, and use initials to identify authors who received the funding. **Describe the role** of any sponsors or funders in the study design, data collection and analysis, decision to publish, or preparation of the manuscript. If they had no role in any of the above, include this sentence at the end of your statement: "*The funders had no role in study design, data collection and analysis, decision to publish, or preparation of the manuscript*." If the study was **unfunded**, provide a statement that clearly indicates this, for example: "*The author(s) received no specific funding for this work*." * typeset	This work was supported by the Swedish Research Council [grant number 521-2011-3205], the Swedish Cancer Society [contract number 11 0600] and the Swedish E-Science Research Centre. The KARMA study was supported by Märit and Hans Rausings Initiative against Breast Cancer and the Cancer Risk Prediction Center (CRisP: www.crispcenter.org), a Linneus Centre [contract number 70867902] financed by the Swedish Research Council. Jingmei Li is supported by the 2nd Joint Council Office (JCO) Career Development Grant (13302EG065).
Competing Interests You are responsible for recognizing and disclosing on behalf of all authors any competing interest that could be perceived to bias their work, acknowledging all financial support and any other relevant financial or non-financial competing interests. Do any authors of this manuscript have competing interests (as described in the PLOS Policy on Declaration and Evaluation of Competing Interests)? **If yes**, please provide details about any and all competing interests in the box below. Your response should begin with this statement: *I have read the journal's policy and the authors of this manuscript have the following competing interests:*	The authors have declared that no competing interests exist.

If no authors have any competing interests to declare, please enter this statement in the box: "*The authors have declared that no competing interests exist.*" * typeset	
Ethics Statement You must provide an ethics statement if your study involved human participants, specimens or tissue samples, or vertebrate animals, embryos or tissues. All information entered here should **also be included in the Methods section** of your manuscript. Please write "N/A" if your study does not require an ethics statement. **Human Subject Research (involved human participants and/or tissue)** All research involving human participants must have been approved by the authors' Institutional Review Board (IRB) or an equivalent committee, and all clinical investigation must have been conducted according to the principles expressed in the Declaration of Helsinki. Informed consent, written or oral, should also have been obtained from the participants. If no consent was given, the reason must be explained (e.g. the data were analyzed anonymously) and reported. The form of consent (written/oral), or reason for lack of consent, should be indicated in the Methods section of your manuscript. Please enter the name of the IRB or Ethics Committee that approved this study in the space below. Include the approval number and/or a statement indicating approval of this research. **Animal Research (involved vertebrate animals, embryos or tissues)** All animal work must have been conducted according to relevant national and international guidelines. If your study involved non-human primates, you must provide details regarding animal welfare and steps taken to ameliorate suffering; this is in accordance with the	All participants provided written informed consent and the study was approved by the ethical review board at the Karolinska Institutet.

recommendations of the Weatherall report, "The use of non-human primates in research." The relevant guidelines followed and the committee that approved the study should be identified in the ethics statement. If anesthesia, euthanasia or any kind of animal sacrifice is part of the study, please include briefly in your statement which substances and/or methods were applied. Please enter the name of your Institutional Animal Care and Use Committee (IACUC) or other relevant ethics board, and indicate whether they approved this research or granted a formal waiver of ethical approval. Also include an approval number if one was obtained. **Field Permit** Please indicate the name of the institution or the relevant body that granted permission.	
Data Availability PLOS journals require authors to make all data underlying the findings described in their manuscript fully available, without restriction and from the time of publication, with only rare exceptions to address legal and ethical concerns (see the PLOS Data Policy and FAQ for further details). When submitting a manuscript, authors must provide a Data Availability Statement that describes where the data underlying their manuscript can be found. Your answers to the following constitute your statement about data availability and will be included with the article in the event of publication. **Please note that simply stating 'data available on request from the author' is not acceptable.** ***If, however, your data are only available upon request from the author(s), you must answer "No" to the first question below, and explain your exceptional situation in the text box provided.*** Do the authors confirm that all data underlying the findings described in their manuscript are fully available without restriction?	Yes - all data are fully available without restriction
Please describe where your data may be	All underlying numerical measurements and data that have been used to derive the

found, writing in full sentences. **Your answers should be entered into the box below and will be published in the form you provide them, if your manuscript is accepted.** If you are copying our sample text below, please ensure you replace any instances of XXX with the appropriate details. If your data are all contained within the paper and/or Supporting Information files, please state this in your answer below. For example, “All relevant data are within the paper and its Supporting Information files.” If your data are held or will be held in a public repository, include URLs, accession numbers or DOIs. For example, “All XXX files are available from the XXX database (accession number(s) XXX, XXX)." If this information will only be available after acceptance, please indicate this by ticking the box below. If neither of these applies but you are able to provide details of access elsewhere, with or without limitations, please do so in the box below. For example: “Data are available from the XXX Institutional Data Access / Ethics Committee for researchers who meet the criteria for access to confidential data.” “Data are from the XXX study whose authors may be contacted at XXX.” * typeset	results in this study are available in the Supporting Information files.
Additional data availability information:	

Area and volumetric density estimation in processed full-field digital mammograms for risk assessment of breast cancer

Abbas Cheddad[1*], Kamila Czene[1], Mikael Eriksson[1], Jingmei Li[2], Douglas Easton[3], Per Hall[1] and Keith Humphreys[1]

[1] Department of Medical Epidemiology and Biostatistics, Karolinska Institutet, Stockholm 171 77, Sweden.[2] Human Genetics, Genome Institute of Singapore, Singapore 138672, Singapore.[3] Centre for Cancer Genetic Epidemiology, Department of Public Health and Primary Care, University of Cambridge, Cambridge, UK.

Short title: Density estimation in processed full-field digital mammograms

Abstract:

Introduction: Mammographic density, the white radiolucent part of a mammogram, is a marker of breast cancer risk and mammographic sensitivity. There are several means of measuring mammographic density, among which are area-based and volumetric-based approaches. Current volumetric methods use only unprocessed, raw, mammograms, which is a problematic restriction since such raw mammograms are normally not stored. We describe fully automated methods for measuring both area and volumetric mammographic density from processed images.

Methods: The data set used in this study comprises raw and processed images of the same view from 1462 women. We developed two algorithms for processed images, an automated area-based approach (CASAM-Area) and a volumetric-based approach (CASAM-Vol). The latter method was based on training a random forest prediction model with image statistical features as predictors, against a volumetric measure, Volpara®, for corresponding raw images. We contrast the three methods, CASAM-Area, CASAM-Vol and Volpara directly and in terms of association with breast cancer risk and a known

genetic variant for mammographic density and breast cancer, *rs10995190* in the gene *ZNF365*. Associations with breast cancer risk were evaluated using images from 47 breast cancer cases and 1011 control subjects. The genetic association analysis was based on 1011 control subjects.

Results: All three measures of mammographic density were associated with breast cancer risk and *rs10995190* ($p < 0.025$ for breast cancer risk and $p < 1\times10^{-6}$ for *rs10995190*). After adjusting for one of the measures there remained little or no evidence of residual association with the remaining density measures ($p > 0.10$ for risk, $p > 0.03$ for *rs10995190*).

Conclusions: Our results show that it is possible to obtain reliable automated measures of volumetric and area mammographic density from processed digital images. Area and volumetric measures of density on processed digital images performed similar in terms of risk and genetic association.

Keywords: Breast cancer risk, Mammographic density, Features, ZNF365, Volpara, FFDM.

* Correspondence: Abbas.Cheddad@ki.se

Introduction

A mammogram is normally used for detection of breast cancers, either in screening or as part of a clinical work up procedure. In recent years there has been intensive research into the information contained in a mammogram in terms of its value in assisting the prediction of breast cancer risk. Breast tissue density is reflected in the amount of fibroglandular tissue that exists in the breast which appears in mammograms as bright areas. The proportion of the total breast area classified as dense tissue is known as percent density (PD) and has been shown to be a strong determinant of breast cancer risk [1,2], independently of other established risk factors.

The classical analog mammogram is essentially a film-based projection of the breast which is mechanically scanned in and digitized (i.e., conversion from analog to digital). For digitized analog images there exists a gold-standard for measuring area density, Cumulus [3]. Although it has been widely used in a research context, its use is not feasible on very large studies or in the clinical setting due to it being semi-automated, i.e., user assisted. We have previously developed an automated procedure which mimics this measure [2] and has been validated and used in research [4,5]. These area-based measures of mammographic density do not take into account the thickness of the dense tissue and rely on a flat two-dimensional projection. Volumetric density can be calculated from screen-film images if a physical phantom, for machine calibration, is placed on the machine's plate at time of mammography, and if acquisition parameters (APs) are recorded. For analog images, a few studies comparing area- and volumetric-density, in terms of breast cancer risk association, have been reported. Their conclusions, however, differ. Boyd et al. [1] found that measurement of the volume of breast tissue did not improve prediction of breast cancer risk as compared to that using an area-based measure. Aitken et al. [6] concluded that area percent density is a stronger predictor of breast cancer risk than the volumetric method SMF (version 2.2ß), whilst Shepherd et al.[7] concluded that volumetric measures of breast density are better predictors of breast cancer risk than percent dense area.

Recent years have seen a shift from analog to full-field digital mammography (FFDM), in which images are acquired directly with high quality. FFDM images are produced in a raw format which gets altered digitally to yield better visualisation. Both *for processing* (*raw*) and *for presentation* (*processed*) images occupy a large memory size. Typically only processed images are stored in the PACS (picture archiving and communication system) [8]. Although there are now FDA cleared algorithms for determining volumetric density on raw digital mammograms, there are few algorithms that measure mammographic density on processed images; that is, the images normally used in clinical settings. Software that needs the raw data (such as computer-aided detection and volumetric breast density algorithms) processes and then deletes the data [9]. Although the semi-automated Cumulus (area-based) approach has been shown to yield correlated area density measurements from raw and processed images [10-13], automating the unification of measurements of processed digital images is a more complicated task than it is on their raw counterparts, owing to the fact that the procedure of processing raw images is not standardised and varies widely by mammography machine vendors who keep the details of their algorithms undisclosed. To use retrospective data sets for mammographic image studies there is a need for algorithms which work well on processed data.

In this article we assess the feasibility of measuring PD from processed FFDM images. We do this using a study in which both raw and processed FFDM images have been collected prospectively. Our approach to volumetric density measurement is based on mimicking Volpara, an FDA cleared algorithm for measuring volumetric density on raw digital mammograms, by combining information on spatial features and acquisition related tags. Additionally, we developed a fully automated approach to measuring area-based density in processed digital images. We compare measurements derived from processed images using our approaches to those obtained from Volpara on corresponding FFDM raw images, directly and in terms of association with breast cancer risk and with the genetic variant, *rs10995190* . All of these comparisons are important and it can even be argued that calibrating density measures against a genetic variant is preferable to using disease status [14]. We also study the importance of individually extracted image

textural features on breast cancer risk and the genetic variant. To the best of our knowledge this is the first article to compare volumetric and area based density on FFDM images in terms of their association with breast cancer risk or a genetic variant for breast cancer/mammographic density. Moreover, we believe that this work forms the first attempt to generate volumetric mammographic density from processed FFDM images without the need for a calibration reference phantom.

Materials and methods

Main study population

All women included in the current study participate in the ***Kar****olinska* ***Ma****mmography* cohort (KARMA) study (http://karmastudy.org/), which is a prospective cohort study that was initiated in January 2011 and comprises women attending mammography screening or clinical mammography at four hospitals in Sweden. Upon study entry, participants donated blood and filled out a detailed web-based questionnaire. In addition, permission was asked for storage of both raw and processed FFDM and linkage to Swedish national registers on inpatient care and cancer. The main analysis presented in this article is based on 47 women diagnosed with incident breast cancer (in KARMA) and 1011 healthy women (in KARMA) with FFDM images (raw and processed, medio-lateral oblique (MLO) images) for the GE Medical Systems, *model:* Senographe Essential version ADS 53.40 and *station name:* HBGMG03. For the 1011 healthy women we have genotype data from iCOGs, a custom illumina iSelect genotyping array designed for replication and fine mapping of common and rare variants with relevance to breast, ovary and prostate cancer [15]. We also had access to the same types of images for an additional 403 healthy women in KARMA (genotype data is not available for these women). Their images were used for developing/training our automated volumetric density measure, CASAM-Vol, to predict Volpara, in a step carried out prior to performing the analysis which used images from the 47 and 1011 women. For the 47

women with breast cancer, all images included in analyses presented here are from the contralateral breast and were taken prior to diagnosis (but less than 3 years prior to diagnosis). For the 1414 healthy women we selected the LMLO view of the image.

Questionnaire data

Information on age, BMI, hormone replacement therapy (HRT) status, reproductive history and other breast cancer risk factors were collected via a web-based questionnaire at study entry. Menopausal status was defined according to information on last year menstruation status, previous oophorectomy and age at study entry.

Ethics Statement

The Karma study has an ethical committee approval by the Ethical Committee at Karolinska Institutet (Dnr 2010/958-31/1) and all participants provided written informed consent.

Measures of PD compared in this study

Volpara (for raw images, version: 1.4.3 | 3433 |): Volpara is an FDA cleared algorithm for measuring volumetric density on both 2D medio-lateral oblique (MLO) and 2D cranio-caudal (CC) raw digital mammograms. The software makes use of the physics information stored with digital mammograms (the acquisition parameters) to work backwards from the pixel intensity values in the raw image to the X-ray attenuation between the pixel and the X-ray source, and uses the X-ray attenuation of an entirely fatty region as an internal reference; see [16,17]. Volumetric percent density is obtained as the ratio of dense volume and breast volume, where dense volume is obtained by summing the dense thickness across all pixels in the breast and breast volume is obtained by multiplying the breast area by the recorded compressed breast thickness, with a correction for the breast edge. By design, Volpara is not extendable to work on processed FFDM or on digitised film mammogram images. That is, its algorithm assumes that

pixel values are proportional to exposure, which is not the case for processed images since the pixel values are non-linearly transformed to enhance the contrast [8]. It is important to know that manufacturers keep the raw-to-processed conversion algorithm secret. A blind reverse engineering of this conversion is not feasible due to non-linearity of the transformation which may be also assisted by some acquisition parameters. Volpara's generated PD is measured on a volumetric scale which is lower than that of area-based PD measures. The approach has recently been demonstrated to correlate well with density measured from magnetic resonance imaging (MRI) images [9,16,17] and a visual assessment method, Breast Imaging-Reporting And Data System (BIRADS) [17]. We use a natural log transformation of Volpara in all analyses presented here which results in values being roughly symmetrically distributed. To date, there have only been a few other attempts to derive volumetric density measures from FFDM images. Heine et al. [18], for example, quantified PD from raw CC images after performing calibration to adjust for inter-image acquisition technique differences.

CASAM-Area (for processed images): CASAM is an acronym for Computer Aided Statistical Assessment of Mammograms. The second density measure assessed here is our own measure of area-based PD on processed mammograms obtained from directly segmenting the breast and fibro-glandular dense tissue areas in the two dimensional space. We have carefully designed our pre-processing steps (of the processed images) in order to arrive at a reliable PD measurement and thereafter to extract meaningful statistical features. In the pre-processing phase we utilised contrast limited adaptive histogram equalization (CLAHE). CASAM-Area takes the square-root of an area-based PD measure. It is calculated as

$$CASAM-Area=\sqrt{\left(\left(\sum_{i=1}^{m}\sum_{j=1}^{n} I(i,j)\in dense\right)/\left(\sum_{i=1}^{m}\sum_{j=1}^{n} I(i,j)\in breast\right)\right)\times 100} \quad (1)$$

where m and n are the dimensions of the image I and *dense* and *breast* refer to segmented regions in the image; see the supplementary material for detailed information about the method.

CASAM-Vol (for processed images): CASAM-Vol is obtained as a weighted combination of statistical and morphological features (measured in processed images) and acquisition related tags, with weights obtained by training a random forest, an ensemble learning nonparametric statistical method for classification and regression developed by Breiman [19], to predict *log* Volpara measurements (from raw images). Images for the subset of 403 women were used for training. The acquisition parameters and statistical/morphological features used for training against Volpara are described in more detail below. We used the pre-compiled MATLAB mex-files [20] to find the optimal value of the shrinkage tuning parameter in which the number of trees was set to 500. Weights obtained from the training data set were subsequently used to produce CASAM-Vol measures, i.e. predicted values of log Volpara, for the processed images from the independent subsets of 47 and 1011 women (the test data). The acquisition parameters, extracted from the image *header*, which we used as inputs to the random forest were: *KVP, XTC (ExposureIn µAs/ ExposureTime), ExposureTime, X-rayTubeCurrent, Exposure, ExposureIn µAs, BodyPartThickness, Log(ExposureIn µAs), (1/ BodyPartThickness), log(BodyPartThickness),(1/ ExposureIn µAs), CompressionForce, AnodeTargetMaterial, RelativeXrayExposure and OrganDose*. We chose to use the acquisition parameters (in addition to features measured in processed images) since they are incorporated into Volpara and are used in the volumetric percent density measure described by [1].

The computer-aided procedure for extracting the features which were used in training CASAM-Vol is described in the supplementary material. The algorithm for pre-processing the processed images was developed to reveal structures within the breast and to lessen the mal-effect of contrast intensity fluctuation. After pre-processing each processed image we segmented the breast region and detected and removed the pectoral muscle. For intra-breast segmentation, uniform thresholding clearly entails knowledge of the intensity values' range, otherwise regions of interests may be missed in the selection process [21] Ch. 3, p. 94. We used a multi-thresholding approach as has been used in [2]. To help circumvent the dense-fatty low contrast issue we apply background subtraction by subtracting the morphologically open image (with a disk-shaped structuring element with a radius of 50 pixels) from its

original image. We then applied 7 thresholding methods to obtain cut-offs from which 12 regions within the breast were determined; see Table S2 in the supplementary material. Finally, a variety of low level and high level features were evaluated comprising 55 measurements for each mammogram (in most cases recalculated for each of the 12 regions, resulting in a feature vector of length 489). The 55 measurements are listed in Table S1.

Genetic data

For the subset of women with iCOGs data we used genotypes for the SNP *rs10995190*, in the gene *ZNF365*. This SNP has been confirmed to be associated with both mammographic density ($p=9\times10^{-10}$) [22] and breast cancer risk ($p=1\times10^{-36}$) [15].

Statistical analysis

To evaluate association between each of the automated PD measures and genotypes of the SNP *rs10995190* (coded 0/1/2, treated as continuous variable), we fitted linear regression models using PD measures one at a time as outcome variables and carried out Wald tests. For CASAM-Area we used the square-root transformation, as in [2,22], to obtain a variable which follows an approximate normal distribution. For Volpara measurements we used a logarithm transform since the distribution of the untransformed measurements are more heavily skewed than the area based measures. In addition to genotype, each model included the variables age (in years) and BMI, menopausal status, HRT use, parity and age at first birth as covariates. We also carried out similar tests of association for each PD measure additionally adjusting for the other PD measures (one at a time).

To explore whether the textural features in Table S1, and the acquisition parameters listed earlier, could be independently associated with *rs10995190* we carried out further association tests (again by fitting

regression models). We first carried out tests adjusting for age, BMI, menopausal status, HRT use, parity and age at first birth, and subsequently additionally adjusting for one other area- or volumetric-PD measure. Each feature was transformed using a Box-Cox transformation (using the *R* package MASS; [23]). $-\text{Log}_{10}$ p-value QQ plots were constructed to summarise the results of these tests using the *R* package Haplin [24]. We also performed a global test of association testing the null hypothesis that none of the features are associated with *rs10995190* after adjusting for PD (Volpara), age and BMI. We first calculated the residuals from fitting regression models with each feature as an outcome (one at a time) and Volpara, age and BMI as covariates. To account for the correlation structure of the features we carried out a permutation (global) test, using as a test statistic the number of p-values < 0.05 from testing association (using a Wald test from a linear regression model) between the residuals and genotypes. We first did this for the observed data and for 10,000 data sets with the genotypes permuted. To obtain our global p-value we compared the value of our global test statistic from the observed data to the distribution of the test statistic from the permuted data sets.

In addition to the genetic association analyses described above we studied the association between the density measures and breast cancer. After combining the data from the subsets of 47 and 1011 women, we evaluated the association between case-control status and the different PD measures using unconditional logistic regression (case/control status as dependent variable and each of the features as the independent variable). As well as adjusting for all potential confounders (used in the genetic analysis), we also carried out analyses with partial adjustment (for age and BMI). We did this because of the small number of cases and to avoid over-adjustment. Finally, we carried out tests of association for each PD measure adjusting for each of the other measures (one at a time) and tested for association with the textural features in Table S1 (using unconditional logistic regression).

R (version 2.13.0) was used for data management, statistical analyses and graphics [25]. All reported tests are two-sided. All of the models were adjusted for age, BMI, menopausal status, HRT use, parity and age at first birth.

Results

Characteristics of the women and their mammographic images, included in each of the data subsets are described in Table 1. No significant differences between the genetic association (control) data set and the cases were observed for the APs, Volpara, CASAM-Area and CASAM-Vol. Differences in age, menopausal status and HRT use were observed but these factors were adjusted for in the case-control analysis (below).

We developed/trained our measure of volumetric density (for processed digital images) using the subset of (raw and processed) images for the 403 women. We also measured area PD in their processed images. Scatter plots of these two sets of measurements against Volpara measurements from corresponding raw images for this training data set are shown in Figure 1 (a). The Pearson's correlation coefficients between Volpara and our PD measures were for CASAM-Area and CASAM-Vol r= 0.77 and r= 0.91, respectively.

We examined the correlation between our measures of PD from processed digital images with Volpara PD measurements (taken from corresponding raw FFDM images), in the subset of 1011 healthy women; see Figure 1 (b). The Pearson's correlation coefficients between Volpara and our PD measures were r= 0.84 and r= 0.91 (CASAM-Area and CASAM-Vol, respectively). From both the training (n= 403) and test (n= 1011) data sets plots, we can assert that it is possible to obtain a reliable volumetric mammographic density from processed images based on predicting Volpara values. Although CASAM-Area and Volpara measures differ conceptually, the correlation between them was observed to be fairly strong (r=0.84).

We next assessed the association between the SNP *rs10995190* and each of the automated PD measures, using our test data sets. All three automated PD measures were associated with *rs10995190*, after adjusting for age, BMI, menopausal status, HRT use, parity and age at first birth ($p<1\times10^{-6}$); see Table 2. As soon as one measure of density was adjusted for, the other measures were, at best, weakly associated with *rs10995190*. There was some evidence that the area and volumetric based approaches complement each other, but only to a very small extent; p=0.036 for the Volpara – *rs10995190* association, after adjusting for CASAM-Area, and p=0.047 for the CASAM-Area – *rs10995190* association after adjusting for Volpara. CASAM-Vol (from processed images) appeared to mimic well Volpara (from raw images) (p=0.079 for the test of "residual" association in Table 3).

We next evaluated association between each of the statistical/textural features and each of the percent density measures. The QQ-plot in Figure 2 (a) shows that the features, as a whole, are strongly associated with *rs10995190* without adjusting for a measure of PD (i.e. with *standard* adjustment for age, BMI, menopausal status, HRT use, parity and age at first birth). After adjusting additionally for Volpara, there remained some evidence of association (Figure 2 (b)). The QQ plots summarising association tests based on adjusting instead for CASAM-Area (Figure 2 (c)) and CASAM-Vol (Figure 2(d)), were similar to those based on adjusting for Volpara. Since the association tests summarised by the QQ-plots are correlated (many of the features and APs are correlated), for the tests based on adjusting for Volpara, we carried out a permutation test of a global null hypothesis (none of the features are associated). We obtained a p-value of 0.047, suggesting that there is some useful information in the images which is not captured by Volpara.

Subsequently, we evaluated the association of PD measurements with cancer risk (case/control status). Table 4 summarises results from fitting logistic regression models with breast cancer status as outcome and PD measurements (one at a time) as a covariate, along with other potential confounders.

After adjusting for one measure of PD, none of the other measures were significantly associated with case-control status ($p>0.10$; Table 5). We tested for association with each of the features listed in Table S1, and each of the APs. The QQ plot summarising the tests which adjusted for Volpara, showed no evidence of association (i.e., no significant deviation from the 45^o line) between the features/APs and case-control status (data not shown).

Discussion

We found the CASAM-based mammographic density measurements to be associated with breast cancer status and *rs10995190* (*ZNF365*), with amount of evidence similar to that found for volumetric measure in raw images (Volpara), suggesting that it is possible to measure density in an automated fashion using processed FFDM images. The p-values from tests of genetic association for the volumetric and area measures were observed to be similar. We found some evidence to suggest that area and volumetric measures of density can complement each other. Our case-control analysis, based on 47 cases, was not able to show that area and volumetric measures of density can complement each other in risk prediction probably due to lack of power. If this can be shown, statistics integrating area and volumetric density should be developed (see [14]). For risk prediction, larger studies are needed to address whether volumetric approaches to breast density measurement in two-dimensional digital images can offer gains over standard area-based measures. Even for analog images it is unclear whether volumetric approaches are markedly better than area approaches [26]. Shepherd et al. [7], however, used digitized film mammograms (275 cases and 825 controls) matched for age, ethnicity, and mammography system, assessed three measures of breast density: PD, fibroglandular volume, and percent fibroglandular volume, and did conclude that volumetric measures of breast density provide more accurate predictors of breast cancer risk than area-based PD.

Approaches for measuring volumetric PD are typically based on calibrating a model against a phantom. Heine et al. used a balloon filled up with water (mimicking the fatty region in a breast) and oil (mimicking the dense region) [27]. Boyd et al. created plastic phantoms representing a range of combinations of fat/fibroglandular tissue to calculate the volumetric percentage density [1]. They based their study on digitized analog films (16 machines in 7 different locations in Canada), all images were CCs (364 cases/656 controls). Breast thickness was recorded under different compression forces along with the thickness read by the machine. Their hypothesis was that the breast thickness reported by a mammography machine needs correction since compression is such that the two used plates will not be perfectly parallel. Additional corrections for exposure and processing were made using a step wedge included in each image. The authors concluded, however, that measurement of the volume of breast tissue, based on utilising APs, in two-dimensional images, did not improve prediction of breast cancer risk over area-based measures. Other researchers have also compared volumetric and area-based measures of PD in two-dimensional images. Ding et al. [28] carried out a large case-control study comprising 634 cases with 1,880 age-matched controls. They used the standard mammography form (SMF) technique to verify the association of the volume of breast density with risk of breast cancer and to compare these measurements with Cumulus readings. SMF uses information about the thickness of the compressed breast, tube voltage and exposure time, to estimate the breast tissue volumes. These volumes were associated with breast cancer risk but less strongly so than the measured area PD (note that Volpara represents an improved version of SMF [13]).

It is possible that the density measures studied in the paper are unable to capture every aspect of density completely. This is supported, in our data, by the fact that the association between rs10995190 and statistical/textural features does not completely disappear after adjusting for these PD measures. No single feature sticks out from the others in terms of its association with *rs10995190* and furthermore it is difficult to interpret individual statistical/textural features in mammographic images [29-31]. The features could relate directly to some biological change in breast composition but, on the other hand, these features could

be capturing some aspect of the X-ray energy that is a proxy for breast composition or dense tissue thickness.

It is clear from Figure 1 that CASAM-Area has a narrower range of values than the conventional area-based methods. This is an inevitable phenomenon since the algorithm encompasses the use of a histogram equaliser called contrast limited adaptive histogram equalization (CLAHE). Applying CLAHE to the mammogram images has significantly increased the accuracy of our algorithm in picking up the dense region within the breast area. This was helpful because CLAHE's underlying algorithm, which is well adopted in medical imaging field, uses a sophisticated adaptive process to enhance image contrast without any saturation occurrences. The reason behind CASAM-Area's lower PD range in Figure 1 being truncated is that CLAHE operation increases the signal-to-noise ratio while highlighting dim structures, in our case that refers to blood vessels in a fatty breast which are classified by our algorithm as dense tissue as one can easily identify by examining Figure S1 (b). On the other hand, the truncation shown in CASAM-Area's upper PD range in Figure 1 could be due to the fact that in a very dense breast, the dense region can be optically exaggerated; making it difficult to distinguish the real dense area border because of the fuzzy gradient contour that arise from an optical occurrence known as the point spread function. By virtue of the properties of CLAHE, the effect of the point spread function is greatly diminished. We believe that our pre-processing and segmentation steps are important for the success of our algorithm, which is why we describe these key steps in some technical details in the supplementary material to provide clarity and to ease replication.

Inclusion of the analysis of association using the genetic variant is a strength of the analysis because case-control association analysis of mammographic images is theoretically susceptible to bias, if there are differences in mammography machines used between cases and controls [14]. For calibrating density measures, it may be better to use genetic variants of mammographic density and breast cancer risk than breast cancer status.

Volpara is cleverly designed to reproduce the volume of breast composition from a 2D projection with high accuracy. However, it works only on raw images and for processed digital images there is no established fully-automated method for measuring density. Although the medical and scientific community are slowly picking up on the value of storing raw images, there are, to date, huge archives of processed digital images which stand to benefit from retrospective assessment of mammographic density for epidemiologic research. Until prospective studies with data from raw images mature, interim measures such as those described in this article could play a vital role in research.

The results of our association analyses using processed FFDM images were similar to those using raw FFDM images, suggesting that processed images may be viable for large-scale epidemiologic research. In this manuscript we have studied three automated measures of mammographic density. The images included here have not been read by a subjective or semi-automatic method. We note, however, that we find that the association between Volpara and Cumulus (an established percent density semi-automatic method) has previously been reported to be high [13] and that Volpara has also been shown to be strongly associated with MRI density measurements (r =0.93) [9]. Quantra (an earlier version of Volpara) has been shown to be associated with the BIRADS classification (89.0% correct classification) [32], and in another recent study Volpara density classification and radiologist's BIRADS showed a positive strong correlation ($r=0.87$; $p<0.001$) [33].

We expect that the PD measures for processed FFDM images, presented here, will perform consistently for mammograms taken from GE machines. There will, however, inevitably be some variability across different vendor machines due to discrepancies in raw-to-processed conversion algorithms. To address this issue, in cohorts comprising mammograms from different vendor machines, it may be necessary to retrain CASAM-Vol to mimic Volpara on each specific machine. Note that CASAM-Vol is constructed from features which include various acquisition parameters that are also exploited by Volpara and are X-ray system dependent (i.e., are not affected by the raw-to-processed conversion algorithm). We expect that

CASAM-Vol can mimic Volpara with similar accuracy across different machines. Brand *et al.* [34] have shown that there are only small differences in distributions of Volpara measurements across different vendor machines. It will therefore probably not be crucial (but it could still be wise) to adjust for machine in case/control or genetic association analyses based on CASAM-Vol. CASAM-Area is more likely, than CASAM-Vol, to be affected by raw-to-processed conversion variability. Like all threshold based methods in the literature, CASAM-Area is image intensity dependent. This intensity is greatly manipulated in an unpredictable way by the raw-to-processed conversion algorithms. For CASAM-Area it will be important to adjust for machines when fitting statistical models in studies incorporating multiple mammography machines.

Abbreviations

PD: percent density; BMI: body mass index; FFDM: Full Field Digital Mammogram; SNP: single-nucleotide polymorphism; CI: confidence interval; CLAHE: contrast limited adaptive histogram equalization; CASAM: Computer Aided Statistical Assessment of Mammograms; MLO: medio-lateral oblique; CC: cranio-caudal; SMF: standard mammography form; APs: acquisition parameters.

Acknowledgements

We thank Aki Tuuliainen for the help in data collection and management.

Authors' contributions

K. Humphreys, A. Cheddad, P. Hall and K. Czene conceived and designed the study. M. Eriksson helped in data collection and management. A. Cheddad and K. Humphreys were responsible for computer programming, data analysis, interpretation and drafting the manuscript. D. Easton and J. Li wrote parts of

the article, and revised it. All authors contributed to manuscript writing and read and approved the final manuscript.

Competing interests

The authors declare that they have no competing interests.

References

1. Boyd N, Martin L, Gunasekara A, Melnichouk O, Maudsley G, et al. (2009) Mammographic density and breast cancer risk: evaluation of a novel method of measuring breast tissue volumes. Cancer Epidemiol Biomarkers Prev 18: 1754-1762.
2. Li J, Szekely L, Eriksson L, Heddson B, Sundbom A, et al. (2012) High-throughput mammographic-density measurement: a tool for risk prediction of breast cancer. Breast Cancer Res 14: R114.
3. Byng JW, Boyd NF, Fishell E, Jong RA, Yaffe MJ (1994) The quantitative analysis of mammographic densities. Phys Med Biol 39: 1629-1638.
4. Li J, Humphreys K, Eriksson L, Edgren G, Czene K, et al. (2013) Mammographic density reduction is a prognostic marker of response to adjuvant tamoxifen therapy in postmenopausal patients with breast cancer. J Clin Oncol 31: 2249-2256.
5. Sandberg ME, Li J, Hall P, Hartman M, dos-Santos-Silva I, et al. (2013) Change of mammographic density predicts the risk of contralateral breast cancer--a case-control study. Breast Cancer Res 15: R57.
6. Aitken Z, McCormack VA, Highnam RP, Martin L, Gunasekara A, et al. (2010) Screen-film mammographic density and breast cancer risk: a comparison of the volumetric standard mammogram form and the interactive threshold measurement methods. Cancer Epidemiol Biomarkers Prev 19: 418-428.
7. Shepherd JA, Kerlikowske K, Ma L, Duewer F, Fan B, et al. (2011) Volume of mammographic density and risk of breast cancer. Cancer Epidemiol Biomarkers Prev 20: 1473-1482.
8. van Engeland S, Snoeren PR, Huisman H, Boetes C, Karssemeijer N (2006) Volumetric breast density estimation from full-field digital mammograms. IEEE Trans Med Imaging 25: 273-282.
9. Gubern-Mérida A, Kallenberg M, Platel B, Mann RM, Martí R, et al. (2014) Volumetric breast density estimation from full-field digital mammograms: a validation study. PLoS One 9: e85952.
10. Vachon CM, Fowler EE, Tiffenberg G, Scott CG, Pankratz VS, et al. (2013) Comparison of percent density from raw and processed full-field digital mammography data. Breast Cancer Res 15: R1.
11. Vachon CM, Kuni CC, Anderson K, Anderson VE, Sellers TA (2000) Association of mammographically defined percent breast density with epidemiologic risk factors for breast cancer (United States). Cancer Causes Control 11: 653-662.
12. Li D, Gavenonis S, Conant E, Kontos D. Comparison of breast percent density estimation from raw versus processed digital mammograms; 2011. *SPIE Proceedings, Medical Imaging: Computer-Aided Diagnosis*. pp. 79631X-79631X-79636.

13. Jeffreys M, Harvey J, Highnam R (2010) Comparing a New Volumetric Breast Density Method (VolparaTM) to Cumulus. In: Martí J, Oliver A, Freixenet J, Martí R, editors. Digital Mammography: Springer Berlin Heidelberg. pp. 408-413.
14. Cheddad A, Czene K, Shepherd JA, Li J, Hall P, et al. (2014) Enhancement of Mammographic Density Measures in Breast Cancer Risk Prediction. Cancer Epidemiol Biomarkers Prev, PMID: 24722754.
15. Michailidou K, Hall P, Gonzalez-Neira A, Ghoussaini M, Dennis J, et al. (2013) Large-scale genotyping identifies 41 new loci associated with breast cancer risk. Nat Genet 45: 353-361, 361e351-352.
16. Highnam R, Brady S, Yaffe M, Karssemeijer N, Harvey J (2010) Robust Breast Composition Measurement - VolparaTM. In: Martí J, Oliver A, Freixenet J, Martí R, editors. Digital Mammography: Springer Berlin Heidelberg. pp. 342-349.
17. Seo JM, Ko ES, Han BK, Ko EY, Shin JH, et al. (2013) Automated volumetric breast density estimation: a comparison with visual assessment. Clin Radiol 68: 690-695.
18. Heine JJ, Cao K, Rollison DE, Tiffenberg G, Thomas JA (2011) A quantitative description of the percentage of breast density measurement using full-field digital mammography. Acad Radiol 18: 556-564.
19. Breiman L (2001) Random Forests. Machine Learning 45: 5-32.
20. Jaiantilal, Abhishek randomforest-matlab. https://code.google.com/p/randomforest-matlab/.
21. Nixon M, S Aguado A (2012) Feature Extraction & Image Processing for Computer Vision: Academic Press.
22. Lindström S, Vachon CM, Li J, Varghese J, Thompson D, et al. (2011) Common variants in ZNF365 are associated with both mammographic density and breast cancer risk. Nat Genet 43: 185-187.
23. Venables B, Ripley B (2002) Modern Applied Statistics with S: Springer.
24. K. Gjessing H (2013) Haplin: Software for genetic association analyses in case-parent triads, case-control data (or combined case-parent control-parent triads), with SNP haplotypes from candidate genes or GWAS data. 5.3 ed.
25. Team TRDC (2010) R: A Language and Environment for Statistical Computing. Version 2.11.1 ed: The R Foundation.
26. Sergeant J, Warwick J, Evans DG, Howell A, Berks M, et al. (2012) Volumetric and Area-Based Breast Density Measurement in the Predicting Risk of Cancer at Screening (PROCAS) Study. In: Maidment AA, Bakic P, Gavenonis S, editors. Breast Imaging: Springer Berlin Heidelberg. pp. 228-235.
27. Heine JJ, Cao K, Thomas JA (2010) Effective radiation attenuation calibration for breast density: compression thickness influences and correction. Biomed Eng Online 9: 73.
28. Ding J, Warren R, Warsi I, Day N, Thompson D, et al. (2008) Evaluating the effectiveness of using standard mammogram form to predict breast cancer risk: case-control study. Cancer Epidemiol Biomarkers Prev 17: 1074-1081.
29. Boyd NF, Martin LJ, Yaffe M, Minkin S (2009) Mammographic density. Breast Cancer Res 11 Suppl 3: S4.
30. Byrne C (1997) Studying mammographic density: implications for understanding breast cancer. J Natl Cancer Inst 89: 531-533.
31. Hofvind S, Geller B, Skaane P (2008) Mammographic features and histopathological findings of interval breast cancers. Acta Radiol 49: 975-981.
32. Ciatto S, Bernardi D, Calabrese M, Durando M, Gentilini MA, et al. (2012) A first evaluation of breast radiological density assessment by QUANTRA software as compared to visual classification. Breast 21: 503-506.
33. McEntee MF, Damases CN. Mammographic density measurement: a comparison of automated volumetric density measurement to BIRADS; 2014. pp. 90370T-90370T-90378.

34. Brand JS, Czene K, Shepherd JA, Leifland K, Heddson B, et al. (2014) Automated Measurement of Volumetric Mammographic Density: A Tool for Widespread Breast Cancer Risk Assessment. Cancer Epidemiol Biomarkers Prev.
35. Gonzalez RC, Woods RE (2008) Digital Image Processing: Pearson.
36. Belkhodja L, Benamrane N. Approche d'extraction de la région globale d'intérêt et suppression des artefacts radiopaques dans une image mammographique; 2009; Biskra, Algeria. *Symposium international: images, multimédias, applications, graphiques et environnements, IMAGE'2009*. pp. 239-248.
37. Pham DL, Xu C, Prince JL (2000) Current methods in medical image segmentation. Annu Rev Biomed Eng 2: 315-337.
38. Cheddad A, Mohamad D, Manaf AA (2008) Exploiting Voronoi diagram properties in face segmentation and feature extraction. Pattern Recognition 41: 3842-3859.
39. Costa L, Cesar R (2001) Shape Analysis and Classification: CRC Press.
40. Wirth MA, Stapinski A. Segmentation of the breast region in mammograms using active contours; 2003. *Proceedings of the SPIE visual communications and image processing*. pp. 1995-2006.
41. Ferrari RJ, Rangayyan RM, Desautels JE, Borges RA, Frère AF (2004) Identification of the breast boundary in mammograms using active contour models. Med Biol Eng Comput 42: 201-208.
42. Berks M (2010) Statistical models for synthesising the appearance of mammographic masses: University of Manchester.
43. Cheddad A, Svensson C, Sharpe J, Georgsson F, Ahlgren U (2012) Image processing assisted algorithms for optical projection tomography. IEEE Trans Med Imaging 31: 1-15.
44. Hörnblad A, Cheddad A, Ahlgren U (2011) An improved protocol for optical projection tomography imaging reveals lobular heterogeneities in pancreatic islet and β-cell mass distribution. Islets 3: 204-208.

Figure Legends

Figure. 1. (a) Scatter-plots of our PD measurements (processed mammograms) and Volpara (raw mammograms) measurements for the training sample of GE mammograms from 403 women (b) scatter-plots of our PD measurements and Volpara measurements for the test sample of GE mammograms from 1011 women with genotype information.

Figure. 2. -$\log_{10}$ QQ plots for p-values assessing the association between the investigated features (Table S1 and APs) and *rs10995190*. (a) with adjustment for age, BMI, menopausal status, HRT use, parity and age at first birth. (b) with adjustment as in *(a)*, plus Volpara. (c) with adjustment as in *(a)*, plus CASAM-Vol. (d) with adjustment as in *(a)*, plus CASAM-Area.

Tables

Table 1: Key characteristics of individuals included in this study (mean (s.d) or n (%)).

	Data used for developing CASAM-Vol (n = 403)	Data used for genetic association study (*) (n=1011)	Cases used for case-control study (n=47)	P-value (ψ) (comparing columns 3&4 data sets)
Age	55.93 (9.12)	53.52 (9.45)	58.59 (8.43)	< 0.001
BMI	25.12(4.17)	25.92 (4.46)	25.67 (4.27)	0.710
Postmenopausal				0.003
No	148 (37)	508 (50)	33 (69)	-
Yes	240 (60)	477 (47)	14 (29)	-
HRT use				0.041
Never	241 (60)	707 (70)	35 (73)	-
Past	102 (25)	204 (20)	6 (13)	-
Current	30 (7)	42 (4)	6 (13)	-
Parity and age at first birth				0.286
Nulliparous	49 (12)	101(10)	9 (19)	-
Parity ≤2 and age at first birth ≤25	95 (24)	250 (25)	13 (27)	-
Parity ≤2 and age at first birth >25	131(33)	380 (38)	16 (33)	-
Parity >2 and age at first birth ≤25	78 (19)	154 (15)	7 (15)	-
Parity >2 and age at first birth >25	35 (9)	99 (10)	2 (4)	-
Acquisition Parameters (APs)				
KVP	29.11 (1.17)	29.44 (1.07)	29.34 (1.13)	0.332
XTC	68.73 (14.75)	66.28 (12.40)	68.57 (14.76)	0.184
ExposureTime	721 (252.86)	819 (316)	767 (293)	0.230
XRayTubeCurrent	68.12 (14.66)	65.68 (12.39)	68.14 (14.82)	0.175
Exposure	47.42 (13.40)	52.59(18.03)	50.37 (15.89)	0.390
ExposureInMicroAs	47403 (13388)	52574 (18023)	50353(15844)	0.377
BodyPartThickness	58.53 (14.53)	61.43 (14.03)	59.02 (14.04)	0.232
AnodeTargetMaterial	0.823 (0.38)	0.884 (0.32)	0.823 (0.38)	0.195
RelativeXrayExposure	4748 (1746)	5426 (2280)	5116 (2025)	0.329
OrganDose	0.010 (0.0022)	0.011 (0.0031)	0.011 (0.0027)	0.277
CompressionForce	102 (29.69)	101 (30)	106 (27.99)	0.209
Volpara (raw)	2.01 (0.56)	2.01 (0.58)	2.12 (0.60)	0.159
CASAM-Area (Processed)	4.58 (1.02)	4.57 (1.03)	4.78 (1.01)	0.160
CASAM-Vol (Processed)	2.01 (0.49)	2.01 (0.50)	2.08 (0.51)	0.393

(*) Also used as controls in the case-control study. (**ψ**) Wald test p-values (logistic regression, unadjusted). (**) LR tests for menopausal status, HRT use and parity.

Table 2: Effect estimates for *rs10995190* on automated measures of mammographic density. Point estimates, interval estimates and p-values (Wald tests) are based on estimated coefficients for the SNP in linear regression models with PD measures as outcomes, adjusting for potential confounding variables (n=1011).

Outcome	Estimate (95%CI)	p-value
Volpara (raw)	-0.138 (-0.191,-0.085)	4×10^{-7}
CASAM-Area (Processed)	-0.254(-0.353,-0.155)	6×10^{-7}
CASAM-Vol (Processed)	-0.113(-0.158,-0.068)	9×10^{-7}

Table 3: p-values assessing the association of the automated measures of mammographic density with *rs10995190* (after additional adjustment for one other density measure) (n=1011).

Outcome variable	Variables adjusted for			
	Standard(*)	Standard+ Volpara	Standard+ CASAM-Area (Processed)	Standard+ CASAM-Vol
Volpara	4×10^{-7}	-	0.036	**0.079**
CASAM-Area (Processed)	6×10^{-7}	0.048	-	**0.147**
CASAM-Vol (Processed)	9×10^{-7}	**0.198**	**0.282**	-

(*) adjusting for age, BMI, menopausal status, HRT use, parity and age at first birth.

Table 4: Effect estimates for automated measures of mammographic density on case-control status, n=1058 (Cases 47, Controls 1011). Point estimates, interval estimates and p-values (Wald tests) are based on estimated coefficients for PD in logistic regression models with case-control status as outcome. (a) with partial adjustment (age and BMI), (b) with full adjustment (age, BMI, menopausal status, HRT use, parity and age at first birth).

Covariate	Estimate (95%CI)	p-value
(a)		
Volpara(raw)	0.978(0.300,1.660)	0.005
CASAM-Area (Processed)	0.483(0.112, 0.862)	0.012
CASAM-Vol (Processed)	0.926 (0.124,1.730)	0.023
(b)		
Volpara(raw)	0.961 (0.239, 1.706)	0.010
CASAM-Area (Processed)	0.467 (0.071, 0.879)	0.023
CASAM-Vol (Processed)	0.813 (-0.041, 1.691)	0.065

528 **Table 5:** p-values assessing the (residual) association between automated measures of mammographic density and
529 case-control status (after adjustment for one other density measure). (a) with partial adjustment (age and BMI), (b)
530 with full adjustment (age, BMI, menopausal status, HRT use, parity and age at first birth) (n=1058).

Covariates			**Variables adjusted for**	
	Standard	Standard+ Volpara	Standard+ CASAM-Area (Processed)	Standard+ CASAM-Vol
(a)				
Volpara	0.005	-	0.479	**0.823**
CASAM-Area (Processed)	0.012	0.162	-	**0.960**
CASAM-Vol (Processed)	0.023	**0.088**	**0.235**	-
(b)				
Volpara	0.010	-	0.529	**0.561**
CASAM-Area (Processed)	0.023	0.172	-	**0.769**
CASAM-Vol (Processed)	0.065	**0.054**	**0.158**	-

531

532

Figure 1
Click here to download high resolution image

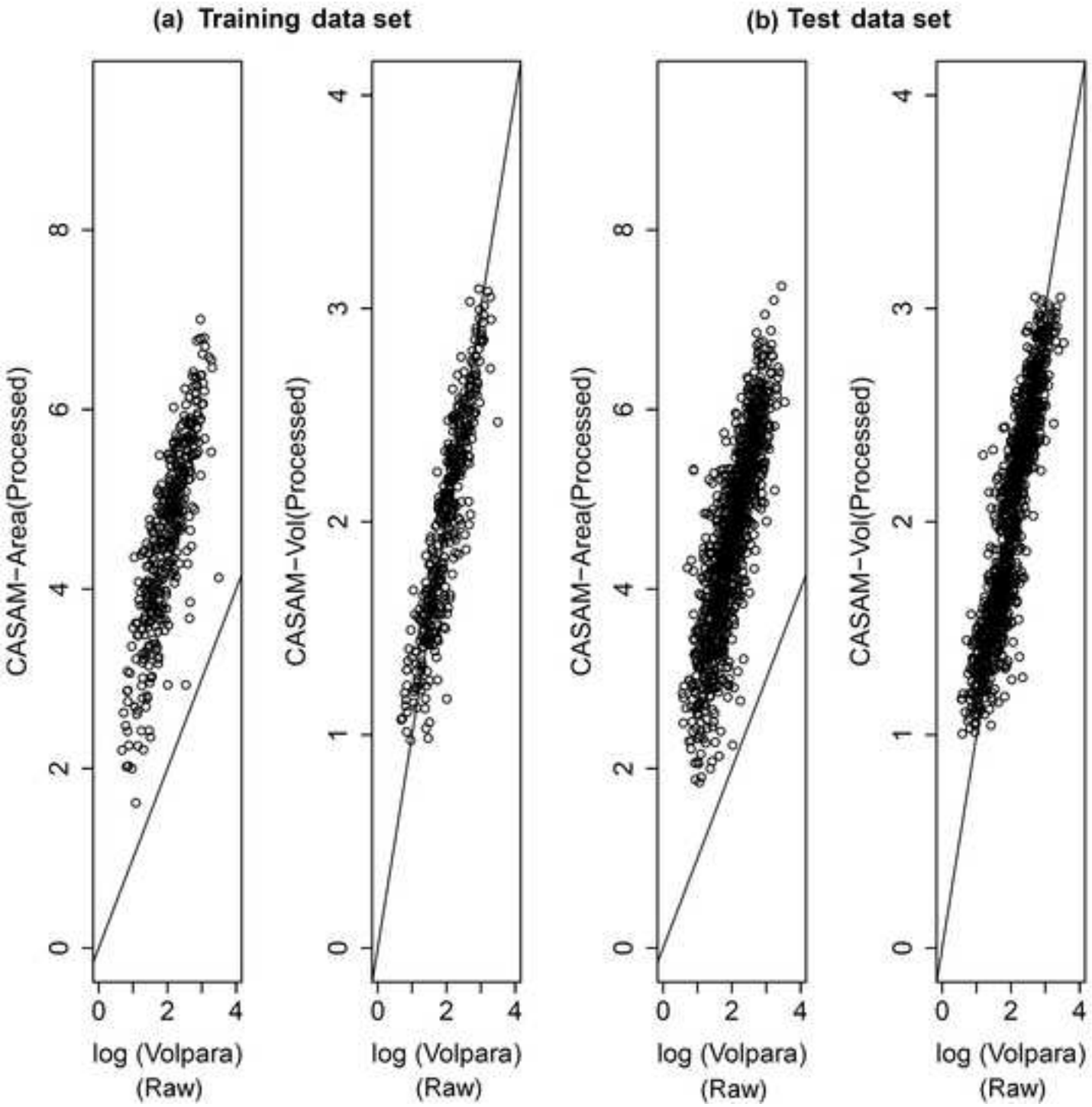

Figure 2
Click here to download high resolution image

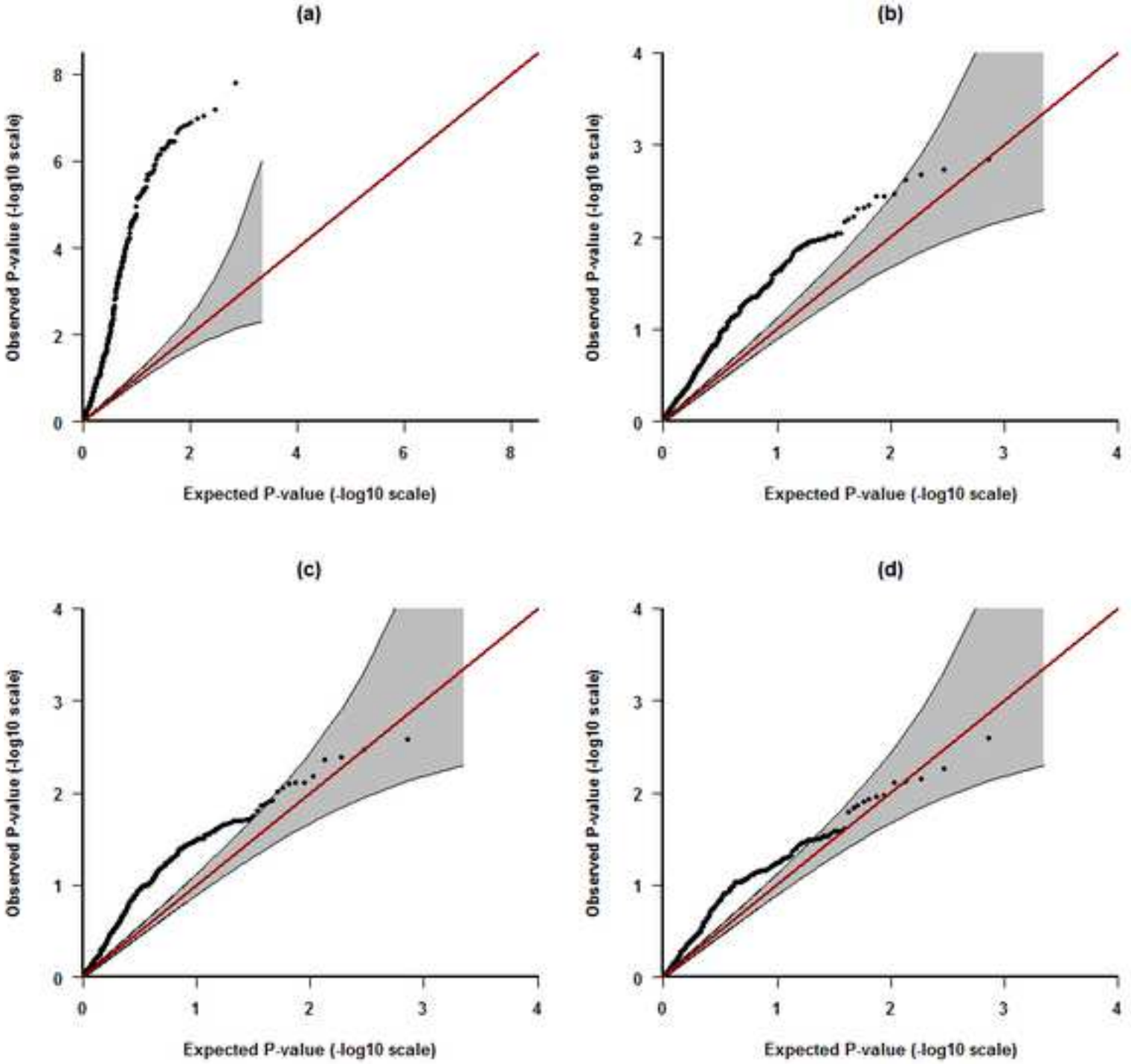

Supporting Information

Click here to download Supporting Information: Supporting Information.docx

Data set

Click here to download Supporting Information: DataForAnalyses.csv

R Code

Click here to download Supporting Information: RCode.txt

Area and volumetric density estimation in processed full-field digital mammograms for risk assessment of breast cancer

Abbas Cheddad[1*], Kamila Czene[1], Mikael Eriksson[1], Jingmei Li[2], Douglas Easton[3], Per Hall[1] and Keith Humphreys[1]

[1] Department of Medical Epidemiology and Biostatistics, Karolinska Institutet, Stockholm 171 77, Sweden.[2] Human Genetics, Genome Institute of Singapore, Singapore 138672, Singapore.[3] Centre for Cancer Genetic Epidemiology, Department of Public Health and Primary Care, University of Cambridge, Cambridge, UK.

Short title: Density estimation in processed full-field digital mammograms

Abstract:

Introduction: Mammographic density, the white radiolucent part of a mammogram, is a marker of breast cancer risk and mammographic sensitivity. There are several means of measuring mammographic density, among which are area-based and volumetric-based approaches. Current volumetric methods use only unprocessed, raw, mammograms, which is a problematic restriction since such raw mammograms are normally not stored. We describe fully automated methods for measuring both area and volumetric mammographic density from processed images.

Methods: The data set used in this study comprises raw and processed images of the same view from 1462 women. We developed two algorithms for processed images, an automated area-based approach (CASAM-Area) and a volumetric-based approach (CASAM-Vol). The latter method was based on training a random forest prediction model with image statistical features as predictors, against a volumetric measure, Volpara®, for corresponding raw images. We contrast the three methods, CASAM-Area, CASAM-Vol and Volpara directly and in terms of association with breast cancer risk and a known

genetic variant for mammographic density and breast cancer, *rs10995190* in the gene *ZNF365*. Associations with breast cancer risk were evaluated using images from 47 breast cancer cases and 1011 control subjects. The genetic association analysis was based on 1011 control subjects.

Results: All three measures of mammographic density were associated with breast cancer risk and *rs10995190* ($p < 0.025$ for breast cancer risk and $p < 1\times10^{-6}$ for *rs10995190*). After adjusting for one of the measures there remained little or no evidence of residual association with the remaining density measures ($p > 0.10$ for risk, $p > 0.03$ for *rs10995190*).

Conclusions: Our results show that it is possible to obtain reliable automated measures of volumetric and area mammographic density from processed digital images. Area and volumetric measures of density on processed digital images performed similar in terms of risk and genetic association.

Keywords: Breast cancer risk, Mammographic density, Features, ZNF365, Volpara, FFDM.

* Correspondence: Abbas.Cheddad@ki.se

Introduction

A mammogram is normally used for detection of breast cancers, either in screening or as part of a clinical work up procedure. In recent years there has been intensive research into the information contained in a mammogram in terms of its value in assisting the prediction of breast cancer risk. Breast tissue density is reflected in the amount of fibroglandular tissue that exists in the breast which appears in mammograms as bright areas. The proportion of the total breast area classified as dense tissue is known as percent density (PD) and has been shown to be a strong determinant of breast cancer risk [1,2], independently of other established risk factors.

The classical analog mammogram is essentially a film-based projection of the breast which is mechanically scanned in and digitized (i.e., conversion from analog to digital). For digitized analog images there exists a gold-standard for measuring area density, Cumulus [3]. Although it has been widely used in a research context, its use is not feasible on very large studies or in the clinical setting due to it being semi-automated, i.e., user assisted. We have previously developed an automated procedure which mimics this measure [2] and has been validated and used in research [4,5]. These area-based measures of mammographic density do not take into account the thickness of the dense tissue and rely on a flat two-dimensional projection. Volumetric density can be calculated from screen-film images if a physical phantom, for machine calibration, is placed on the machine's plate at time of mammography, and if acquisition parameters (APs) are recorded. For analog images, a few studies comparing area- and volumetric-density, in terms of breast cancer risk association, have been reported. Their conclusions, however, differ. Boyd et al. [1] found that measurement of the volume of breast tissue did not improve prediction of breast cancer risk as compared to that using an area-based measure. Aitken et al. [6] concluded that area percent density is a stronger predictor of breast cancer risk than the volumetric method SMF (version 2.2ß), whilst Shepherd et al.[7] concluded that volumetric measures of breast density are better predictors of breast cancer risk than percent dense area.

Recent years have seen a shift from analog to full-field digital mammography (FFDM), in which images are acquired directly with high quality. FFDM images are produced in a raw format which gets altered digitally to yield better visualisation. Both *for processing* (*raw*) and *for presentation* (*processed*) images occupy a large memory size. Typically only processed images are stored in the PACS (picture archiving and communication system) [8]. Although there are now FDA cleared algorithms for determining volumetric density on raw digital mammograms, there are few algorithms that measure mammographic density on processed images; that is, the images normally used in clinical settings. Software that needs the raw data (such as computer-aided detection and volumetric breast density algorithms) processes and then deletes the data [9]. Although the semi-automated Cumulus (area-based) approach has been shown to yield correlated area density measurements from raw and processed images [10-13], automating the unification of measurements of processed digital images is a more complicated task than it is on their raw counterparts, owing to the fact that the procedure of processing raw images is not standardised and varies widely by mammography machine vendors who keep the details of their algorithms undisclosed. To use retrospective data sets for mammographic image studies there is a need for algorithms which work well on processed data.

In this article we assess the feasibility of measuring PD from processed FFDM images. We do this using a study in which both raw and processed FFDM images have been collected prospectively. Our approach to volumetric density measurement is based on mimicking Volpara, an FDA cleared algorithm for measuring volumetric density on raw digital mammograms, by combining information on spatial features and acquisition related tags. Additionally, we developed a fully automated approach to measuring area-based density in processed digital images. We compare measurements derived from processed images using our approaches to those obtained from Volpara on corresponding FFDM raw images, directly and in terms of association with breast cancer risk and with the genetic variant, *rs10995190* . All of these comparisons are important and it can even be argued that calibrating density measures against a genetic variant is preferable to using disease status [14]. We also study the importance of individually extracted image

textural features on breast cancer risk and the genetic variant. To the best of our knowledge this is the first article to compare volumetric and area based density on FFDM images in terms of their association with breast cancer risk or a genetic variant for breast cancer/mammographic density. Moreover, we believe that this work forms the first attempt to generate volumetric mammographic density from processed FFDM images without the need for a calibration reference phantom.

Materials and methods

Main study population

All women included in the current study participate in the ***Kar****olinska* ***Ma****mmography* cohort (KARMA) study (http://karmastudy.org/), which is a prospective cohort study that was initiated in January 2011 and comprises women attending mammography screening or clinical mammography at four hospitals in Sweden. Upon study entry, participants donated blood and filled out a detailed web-based questionnaire. In addition, permission was asked for storage of both raw and processed FFDM and linkage to Swedish national registers on inpatient care and cancer. The main analysis presented in this article is based on 47 women diagnosed with incident breast cancer (in KARMA) and 1011 healthy women (in KARMA) with FFDM images (raw and processed, medio-lateral oblique (MLO) images) for the GE Medical Systems, *model:* Senographe Essential version ADS 53.40 and *station name:* HBGMG03. For the 1011 healthy women we have genotype data from iCOGs, a custom illumina iSelect genotyping array designed for replication and fine mapping of common and rare variants with relevance to breast, ovary and prostate cancer [15]. We also had access to the same types of images for an additional 403 healthy women in KARMA (genotype data is not available for these women). Their images were used for developing/training our automated volumetric density measure, CASAM-Vol, to predict Volpara, in a step carried out prior to performing the analysis which used images from the 47 and 1011 women. For the 47

113 women with breast cancer, all images included in analyses presented here are from the contralateral breast
114 and were taken prior to diagnosis (but less than 3 years prior to diagnosis). For the 1414 healthy women
115 we selected the LMLO view of the image.

116 Questionnaire data

117 Information on age, BMI, hormone replacement therapy (HRT) status, reproductive history and other
118 breast cancer risk factors were collected via a web-based questionnaire at study entry. Menopausal status
119 was defined according to information on last year menstruation status, previous oophorectomy and age at
120 study entry.

121 Ethics Statement

122 The Karma study has an ethical committee approval by the Ethical Committee at Karolinska Institutet
123 (Dnr 2010/958-31/1) and all participants provided written informed consent.

124 Measures of PD compared in this study

125 *Volpara* (for raw images, version: 1.4.3 | 3433 |): Volpara is an FDA cleared algorithm for measuring
126 volumetric density on both 2D medio-lateral oblique (MLO) and 2D cranio-caudal (CC) raw digital
127 mammograms. The software makes use of the physics information stored with digital mammograms (the
128 acquisition parameters) to work backwards from the pixel intensity values in the raw image to the X-ray
129 attenuation between the pixel and the X-ray source, and uses the X-ray attenuation of an entirely fatty
130 region as an internal reference; see [16,17]. Volumetric percent density is obtained as the ratio of dense
131 volume and breast volume, where dense volume is obtained by summing the dense thickness across all
132 pixels in the breast and breast volume is obtained by multiplying the breast area by the recorded
133 compressed breast thickness, with a correction for the breast edge. By design, Volpara is not extendable to
134 work on processed FFDM or on digitised film mammogram images. That is, its algorithm assumes that

pixel values are proportional to exposure, which is not the case for processed images since the pixel values are non-linearly transformed to enhance the contrast [8]. It is important to know that manufacturers keep the raw-to-processed conversion algorithm secret. A blind reverse engineering of this conversion is not feasible due to non-linearity of the transformation which may be also assisted by some acquisition parameters. Volpara's generated PD is measured on a volumetric scale which is lower than that of area-based PD measures. The approach has recently been demonstrated to correlate well with density measured from magnetic resonance imaging (MRI) images [9,16,17] and a visual assessment method, Breast Imaging-Reporting And Data System (BIRADS) [17]. We use a natural log transformation of Volpara in all analyses presented here which results in values being roughly symmetrically distributed. To date, there have only been a few other attempts to derive volumetric density measures from FFDM images. Heine et al. [18], for example, quantified PD from raw CC images after performing calibration to adjust for inter-image acquisition technique differences.

CASAM-Area (for processed images): CASAM is an acronym for Computer Aided Statistical Assessment of Mammograms. The second density measure assessed here is our own measure of area-based PD on processed mammograms obtained from directly segmenting the breast and fibro-glandular dense tissue areas in the two dimensional space. We have carefully designed our pre-processing steps (of the processed images) in order to arrive at a reliable PD measurement and thereafter to extract meaningful statistical features. In the pre-processing phase we utilised contrast limited adaptive histogram equalization (CLAHE). CASAM-Area takes the square-root of an area-based PD measure. It is calculated as

$$CASAM-Area=\sqrt{\left(\left(\sum_{i=1}^{m}\sum_{j=1}^{n} I(i,j)\in dense\right)/\left(\sum_{i=1}^{m}\sum_{j=1}^{n} I(i,j)\in breast\right)\right)\times 100} \quad (1)$$

where m and n are the dimensions of the image I and *dense* and *breast* refer to segmented regions in the image; see the supplementary material for detailed information about the method.

CASAM-Vol (for processed images): CASAM-Vol is obtained as a weighted combination of statistical and morphological features (measured in processed images) and acquisition related tags, with weights obtained by training a random forest, an ensemble learning nonparametric statistical method for classification and regression developed by Breiman [19], to predict *log* Volpara measurements (from raw images). Images for the subset of 403 women were used for training. The acquisition parameters and statistical/morphological features used for training against Volpara are described in more detail below. We used the pre-compiled MATLAB mex-files [20] to find the optimal value of the shrinkage tuning parameter in which the number of trees was set to 500. Weights obtained from the training data set were subsequently used to produce CASAM-Vol measures, i.e. predicted values of log Volpara, for the processed images from the independent subsets of 47 and 1011 women (the test data). The acquisition parameters, extracted from the image *header*, which we used as inputs to the random forest were: *KVP, XTC (ExposureIn µAs/ ExposureTime), ExposureTime, X-rayTubeCurrent, Exposure, ExposureIn µAs, BodyPartThickness, Log(ExposureIn µAs), (1/ BodyPartThickness), log(BodyPartThickness),(1/ ExposureIn µAs), CompressionForce, AnodeTargetMaterial, RelativeXrayExposure and OrganDose*. We chose to use the acquisition parameters (in addition to features measured in processed images) since they are incorporated into Volpara and are used in the volumetric percent density measure described by [1].

The computer-aided procedure for extracting the features which were used in training CASAM-Vol is described in the supplementary material. The algorithm for pre-processing the processed images was developed to reveal structures within the breast and to lessen the mal-effect of contrast intensity fluctuation. After pre-processing each processed image we segmented the breast region and detected and removed the pectoral muscle. For intra-breast segmentation, uniform thresholding clearly entails knowledge of the intensity values' range, otherwise regions of interests may be missed in the selection process [21] Ch. 3, p. 94. We used a multi-thresholding approach as has been used in [2]. To help circumvent the dense-fatty low contrast issue we apply background subtraction by subtracting the morphologically open image (with a disk-shaped structuring element with a radius of 50 pixels) from its

original image. We then applied 7 thresholding methods to obtain cut-offs from which 12 regions within the breast were determined; see Table S2 in the supplementary material. Finally, a variety of low level and high level features were evaluated comprising 55 measurements for each mammogram (in most cases recalculated for each of the 12 regions, resulting in a feature vector of length 489). The 55 measurements are listed in Table S1.

Genetic data

For the subset of women with iCOGs data we used genotypes for the SNP *rs10995190*, in the gene *ZNF365*. This SNP has been confirmed to be associated with both mammographic density ($p=9\times10^{-10}$) [22] and breast cancer risk ($p=1\times10^{-36}$) [15].

Statistical analysis

To evaluate association between each of the automated PD measures and genotypes of the SNP *rs10995190* (coded 0/1/2, treated as continuous variable), we fitted linear regression models using PD measures one at a time as outcome variables and carried out Wald tests. For CASAM-Area we used the square-root transformation, as in [2,22], to obtain a variable which follows an approximate normal distribution. For Volpara measurements we used a logarithm transform since the distribution of the untransformed measurements are more heavily skewed than the area based measures. In addition to genotype, each model included the variables age (in years) and BMI, menopausal status, HRT use, parity and age at first birth as covariates. We also carried out similar tests of association for each PD measure additionally adjusting for the other PD measures (one at a time).

To explore whether the textural features in Table S1, and the acquisition parameters listed earlier, could be independently associated with *rs10995190* we carried out further association tests (again by fitting

regression models). We first carried out tests adjusting for age, BMI, menopausal status, HRT use, parity and age at first birth, and subsequently additionally adjusting for one other area- or volumetric-PD measure. Each feature was transformed using a Box-Cox transformation (using the *R* package MASS; [23]). $-\text{Log}_{10}$ p-value QQ plots were constructed to summarise the results of these tests using the *R* package Haplin [24]. We also performed a global test of association testing the null hypothesis that none of the features are associated with *rs10995190* after adjusting for PD (Volpara), age and BMI. We first calculated the residuals from fitting regression models with each feature as an outcome (one at a time) and Volpara, age and BMI as covariates. To account for the correlation structure of the features we carried out a permutation (global) test, using as a test statistic the number of p-values < 0.05 from testing association (using a Wald test from a linear regression model) between the residuals and genotypes. We first did this for the observed data and for 10,000 data sets with the genotypes permuted. To obtain our global p-value we compared the value of our global test statistic from the observed data to the distribution of the test statistic from the permuted data sets.

In addition to the genetic association analyses described above we studied the association between the density measures and breast cancer. After combining the data from the subsets of 47 and 1011 women, we evaluated the association between case-control status and the different PD measures using unconditional logistic regression (case/control status as dependent variable and each of the features as the independent variable). As well as adjusting for all potential confounders (used in the genetic analysis), we also carried out analyses with partial adjustment (for age and BMI). We did this because of the small number of cases and to avoid over-adjustment. Finally, we carried out tests of association for each PD measure adjusting for each of the other measures (one at a time) and tested for association with the textural features in Table S1 (using unconditional logistic regression).

R (version 2.13.0) was used for data management, statistical analyses and graphics [25]. All reported tests are two-sided. All of the models were adjusted for age, BMI, menopausal status, HRT use, parity and age at first birth.

Results

Characteristics of the women and their mammographic images, included in each of the data subsets are described in Table 1. No significant differences between the genetic association (control) data set and the cases were observed for the APs, Volpara, CASAM-Area and CASAM-Vol. Differences in age, menopausal status and HRT use were observed but these factors were adjusted for in the case-control analysis (below).

We developed/trained our measure of volumetric density (for processed digital images) using the subset of (raw and processed) images for the 403 women. We also measured area PD in their processed images. Scatter plots of these two sets of measurements against Volpara measurements from corresponding raw images for this training data set are shown in Figure 1 (a). The Pearson's correlation coefficients between Volpara and our PD measures were for CASAM-Area and CASAM-Vol r= 0.77 and r= 0.91, respectively.

We examined the correlation between our measures of PD from processed digital images with Volpara PD measurements (taken from corresponding raw FFDM images), in the subset of 1011 healthy women; see Figure 1 (b). The Pearson's correlation coefficients between Volpara and our PD measures were r= 0.84 and r= 0.91 (CASAM-Area and CASAM-Vol, respectively). From both the training (n= 403) and test (n= 1011) data sets plots, we can assert that it is possible to obtain a reliable volumetric mammographic density from processed images based on predicting Volpara values. Although CASAM-Area and Volpara measures differ conceptually, the correlation between them was observed to be fairly strong (r=0.84).

We next assessed the association between the SNP *rs10995190* and each of the automated PD measures, using our test data sets. All three automated PD measures were associated with *rs10995190*, after adjusting for age, BMI, menopausal status, HRT use, parity and age at first birth ($p<1\times10^{-6}$); see Table 2. As soon as one measure of density was adjusted for, the other measures were, at best, weakly associated with *rs10995190*. There was some evidence that the area and volumetric based approaches complement each other, but only to a very small extent; p=0.036 for the Volpara – *rs10995190* association, after adjusting for CASAM-Area, and p=0.047 for the CASAM-Area – *rs10995190* association after adjusting for Volpara. CASAM-Vol (from processed images) appeared to mimic well Volpara (from raw images) (p=0.079 for the test of "residual" association in Table 3).

We next evaluated association between each of the statistical/textural features and each of the percent density measures. The QQ-plot in Figure 2 (a) shows that the features, as a whole, are strongly associated with *rs10995190* without adjusting for a measure of PD (i.e. with *standard* adjustment for age, BMI, menopausal status, HRT use, parity and age at first birth). After adjusting additionally for Volpara, there remained some evidence of association (Figure 2 (b)). The QQ plots summarising association tests based on adjusting instead for CASAM-Area (Figure 2 (c)) and CASAM-Vol (Figure 2(d)), were similar to those based on adjusting for Volpara. Since the association tests summarised by the QQ-plots are correlated (many of the features and APs are correlated), for the tests based on adjusting for Volpara, we carried out a permutation test of a global null hypothesis (none of the features are associated). We obtained a p-value of 0.047, suggesting that there is some useful information in the images which is not captured by Volpara.

Subsequently, we evaluated the association of PD measurements with cancer risk (case/control status). Table 4 summarises results from fitting logistic regression models with breast cancer status as outcome and PD measurements (one at a time) as a covariate, along with other potential confounders.

After adjusting for one measure of PD, none of the other measures were significantly associated with case-control status ($p>0.10$; Table 5). We tested for association with each of the features listed in Table S1, and each of the APs. The QQ plot summarising the tests which adjusted for Volpara, showed no evidence of association (i.e., no significant deviation from the 45^{o} line) between the features/APs and case-control status (data not shown).

Discussion

We found the CASAM-based mammographic density measurements to be associated with breast cancer status and *rs10995190* (*ZNF365*), with amount of evidence similar to that found for volumetric measure in raw images (Volpara), suggesting that it is possible to measure density in an automated fashion using processed FFDM images. The p-values from tests of genetic association for the volumetric and area measures were observed to be similar. We found some evidence to suggest that area and volumetric measures of density can complement each other. Our case-control analysis, based on 47 cases, was not able to show that area and volumetric measures of density can complement each other in risk prediction probably due to lack of power. If this can be shown, statistics integrating area and volumetric density should be developed (see [14]). For risk prediction, larger studies are needed to address whether volumetric approaches to breast density measurement in two-dimensional digital images can offer gains over standard area-based measures. Even for analog images it is unclear whether volumetric approaches are markedly better than area approaches [26]. Shepherd et al. [7], however, used digitized film mammograms (275 cases and 825 controls) matched for age, ethnicity, and mammography system, assessed three measures of breast density: PD, fibroglandular volume, and percent fibroglandular volume, and did conclude that volumetric measures of breast density provide more accurate predictors of breast cancer risk than area-based PD.

Approaches for measuring volumetric PD are typically based on calibrating a model against a phantom. Heine et al. used a balloon filled up with water (mimicking the fatty region in a breast) and oil (mimicking the dense region) [27]. Boyd et al. created plastic phantoms representing a range of combinations of fat/fibroglandular tissue to calculate the volumetric percentage density [1]. They based their study on digitized analog films (16 machines in 7 different locations in Canada), all images were CCs (364 cases/656 controls). Breast thickness was recorded under different compression forces along with the thickness read by the machine. Their hypothesis was that the breast thickness reported by a mammography machine needs correction since compression is such that the two used plates will not be perfectly parallel. Additional corrections for exposure and processing were made using a step wedge included in each image. The authors concluded, however, that measurement of the volume of breast tissue, based on utilising APs, in two-dimensional images, did not improve prediction of breast cancer risk over area-based measures. Other researchers have also compared volumetric and area-based measures of PD in two-dimensional images. Ding et al. [28] carried out a large case-control study comprising 634 cases with 1,880 age-matched controls. They used the standard mammography form (SMF) technique to verify the association of the volume of breast density with risk of breast cancer and to compare these measurements with Cumulus readings. SMF uses information about the thickness of the compressed breast, tube voltage and exposure time, to estimate the breast tissue volumes. These volumes were associated with breast cancer risk but less strongly so than the measured area PD (note that Volpara represents an improved version of SMF [13]).

It is possible that the density measures studied in the paper are unable to capture every aspect of density completely. This is supported, in our data, by the fact that the association between rs10995190 and statistical/textural features does not completely disappear after adjusting for these PD measures. No single feature sticks out from the others in terms of its association with *rs10995190* and furthermore it is difficult to interpret individual statistical/textural features in mammographic images [29-31]. The features could relate directly to some biological change in breast composition but, on the other hand, these features could

be capturing some aspect of the X-ray energy that is a proxy for breast composition or dense tissue thickness.

It is clear from Figure 1 that CASAM-Area has a narrower range of values than the conventional area-based methods. This is an inevitable phenomenon since the algorithm encompasses the use of a histogram equaliser called contrast limited adaptive histogram equalization (CLAHE). Applying CLAHE to the mammogram images has significantly increased the accuracy of our algorithm in picking up the dense region within the breast area. This was helpful because CLAHE's underlying algorithm, which is well adopted in medical imaging field, uses a sophisticated adaptive process to enhance image contrast without any saturation occurrences. The reason behind CASAM-Area's lower PD range in Figure 1 being truncated is that CLAHE operation increases the signal-to-noise ratio while highlighting dim structures, in our case that refers to blood vessels in a fatty breast which are classified by our algorithm as dense tissue as one can easily identify by examining Figure S1 (b). On the other hand, the truncation shown in CASAM-Area's upper PD range in Figure 1 could be due to the fact that in a very dense breast, the dense region can be optically exaggerated; making it difficult to distinguish the real dense area border because of the fuzzy gradient contour that arise from an optical occurrence known as the point spread function. By virtue of the properties of CLAHE, the effect of the point spread function is greatly diminished. We believe that our pre-processing and segmentation steps are important for the success of our algorithm, which is why we describe these key steps in some technical details in the supplementary material to provide clarity and to ease replication.

Inclusion of the analysis of association using the genetic variant is a strength of the analysis because case-control association analysis of mammographic images is theoretically susceptible to bias, if there are differences in mammography machines used between cases and controls [14]. For calibrating density measures, it may be better to use genetic variants of mammographic density and breast cancer risk than breast cancer status.

Volpara is cleverly designed to reproduce the volume of breast composition from a 2D projection with high accuracy. However, it works only on raw images and for processed digital images there is no established fully-automated method for measuring density. Although the medical and scientific community are slowly picking up on the value of storing raw images, there are, to date, huge archives of processed digital images which stand to benefit from retrospective assessment of mammographic density for epidemiologic research. Until prospective studies with data from raw images mature, interim measures such as those described in this article could play a vital role in research.

The results of our association analyses using processed FFDM images were similar to those using raw FFDM images, suggesting that processed images may be viable for large-scale epidemiologic research. In this manuscript we have studied three automated measures of mammographic density. The images included here have not been read by a subjective or semi-automatic method. We note, however, that we find that the association between Volpara and Cumulus (an established percent density semi-automatic method) has previously been reported to be high [13] and that Volpara has also been shown to be strongly associated with MRI density measurements (r =0.93) [9]. Quantra (an earlier version of Volpara) has been shown to be associated with the BIRADS classification (89.0% correct classification) [32], and in another recent study Volpara density classification and radiologist's BIRADS showed a positive strong correlation ($r=0.87$; $p<0.001$) [33].

We expect that the PD measures for processed FFDM images, presented here, will perform consistently for mammograms taken from GE machines. There will, however, inevitably be some variability across different vendor machines due to discrepancies in raw-to-processed conversion algorithms. To address this issue, in cohorts comprising mammograms from different vendor machines, it may be necessary to retrain CASAM-Vol to mimic Volpara on each specific machine. Note that CASAM-Vol is constructed from features which include various acquisition parameters that are also exploited by Volpara and are X-ray system dependent (i.e., are not affected by the raw-to-processed conversion algorithm). We expect that

CASAM-Vol can mimic Volpara with similar accuracy across different machines. Brand *et al.* [34] have shown that there are only small differences in distributions of Volpara measurements across different vendor machines. It will therefore probably not be crucial (but it could still be wise) to adjust for machine in case/control or genetic association analyses based on CASAM-Vol. CASAM-Area is more likely, than CASAM-Vol, to be affected by raw-to-processed conversion variability. Like all threshold based methods in the literature, CASAM-Area is image intensity dependent. This intensity is greatly manipulated in an unpredictable way by the raw-to-processed conversion algorithms. For CASAM-Area it will be important to adjust for machines when fitting statistical models in studies incorporating multiple mammography machines.

Abbreviations

PD: percent density; BMI: body mass index; FFDM: Full Field Digital Mammogram; SNP: single-nucleotide polymorphism; CI: confidence interval; CLAHE: contrast limited adaptive histogram equalization; CASAM: Computer Aided Statistical Assessment of Mammograms; MLO: medio-lateral oblique; CC: cranio-caudal; SMF: standard mammography form; APs: acquisition parameters.

Acknowledgements

We thank Aki Tuuliainen for the help in data collection and management.

Authors' contributions

K. Humphreys, A. Cheddad, P. Hall and K. Czene conceived and designed the study. M. Eriksson helped in data collection and management. A. Cheddad and K. Humphreys were responsible for computer programming, data analysis, interpretation and drafting the manuscript. D. Easton and J. Li wrote parts of

the article, and revised it. All authors contributed to manuscript writing and read and approved the final manuscript.

Competing interests

The authors declare that they have no competing interests.

References

1. Boyd N, Martin L, Gunasekara A, Melnichouk O, Maudsley G, et al. (2009) Mammographic density and breast cancer risk: evaluation of a novel method of measuring breast tissue volumes. Cancer Epidemiol Biomarkers Prev 18: 1754-1762.
2. Li J, Szekely L, Eriksson L, Heddson B, Sundbom A, et al. (2012) High-throughput mammographic-density measurement: a tool for risk prediction of breast cancer. Breast Cancer Res 14: R114.
3. Byng JW, Boyd NF, Fishell E, Jong RA, Yaffe MJ (1994) The quantitative analysis of mammographic densities. Phys Med Biol 39: 1629-1638.
4. Li J, Humphreys K, Eriksson L, Edgren G, Czene K, et al. (2013) Mammographic density reduction is a prognostic marker of response to adjuvant tamoxifen therapy in postmenopausal patients with breast cancer. J Clin Oncol 31: 2249-2256.
5. Sandberg ME, Li J, Hall P, Hartman M, dos-Santos-Silva I, et al. (2013) Change of mammographic density predicts the risk of contralateral breast cancer--a case-control study. Breast Cancer Res 15: R57.
6. Aitken Z, McCormack VA, Highnam RP, Martin L, Gunasekara A, et al. (2010) Screen-film mammographic density and breast cancer risk: a comparison of the volumetric standard mammogram form and the interactive threshold measurement methods. Cancer Epidemiol Biomarkers Prev 19: 418-428.
7. Shepherd JA, Kerlikowske K, Ma L, Duewer F, Fan B, et al. (2011) Volume of mammographic density and risk of breast cancer. Cancer Epidemiol Biomarkers Prev 20: 1473-1482.
8. van Engeland S, Snoeren PR, Huisman H, Boetes C, Karssemeijer N (2006) Volumetric breast density estimation from full-field digital mammograms. IEEE Trans Med Imaging 25: 273-282.
9. Gubern-Mérida A, Kallenberg M, Platel B, Mann RM, Martí R, et al. (2014) Volumetric breast density estimation from full-field digital mammograms: a validation study. PLoS One 9: e85952.
10. Vachon CM, Fowler EE, Tiffenberg G, Scott CG, Pankratz VS, et al. (2013) Comparison of percent density from raw and processed full-field digital mammography data. Breast Cancer Res 15: R1.
11. Vachon CM, Kuni CC, Anderson K, Anderson VE, Sellers TA (2000) Association of mammographically defined percent breast density with epidemiologic risk factors for breast cancer (United States). Cancer Causes Control 11: 653-662.
12. Li D, Gavenonis S, Conant E, Kontos D. Comparison of breast percent density estimation from raw versus processed digital mammograms; 2011. *SPIE Proceedings, Medical Imaging: Computer-Aided Diagnosis*. pp. 79631X-79631X-79636.

13. Jeffreys M, Harvey J, Highnam R (2010) Comparing a New Volumetric Breast Density Method (VolparaTM) to Cumulus. In: Martí J, Oliver A, Freixenet J, Martí R, editors. Digital Mammography: Springer Berlin Heidelberg. pp. 408-413.
14. Cheddad A, Czene K, Shepherd JA, Li J, Hall P, et al. (2014) Enhancement of Mammographic Density Measures in Breast Cancer Risk Prediction. Cancer Epidemiol Biomarkers Prev, PMID: 24722754.
15. Michailidou K, Hall P, Gonzalez-Neira A, Ghoussaini M, Dennis J, et al. (2013) Large-scale genotyping identifies 41 new loci associated with breast cancer risk. Nat Genet 45: 353-361, 361e351-352.
16. Highnam R, Brady S, Yaffe M, Karssemeijer N, Harvey J (2010) Robust Breast Composition Measurement - VolparaTM. In: Martí J, Oliver A, Freixenet J, Martí R, editors. Digital Mammography: Springer Berlin Heidelberg. pp. 342-349.
17. Seo JM, Ko ES, Han BK, Ko EY, Shin JH, et al. (2013) Automated volumetric breast density estimation: a comparison with visual assessment. Clin Radiol 68: 690-695.
18. Heine JJ, Cao K, Rollison DE, Tiffenberg G, Thomas JA (2011) A quantitative description of the percentage of breast density measurement using full-field digital mammography. Acad Radiol 18: 556-564.
19. Breiman L (2001) Random Forests. Machine Learning 45: 5-32.
20. Jaiantilal, Abhishek randomforest-matlab. https://code.google.com/p/randomforest-matlab/.
21. Nixon M, S Aguado A (2012) Feature Extraction & Image Processing for Computer Vision: Academic Press.
22. Lindström S, Vachon CM, Li J, Varghese J, Thompson D, et al. (2011) Common variants in ZNF365 are associated with both mammographic density and breast cancer risk. Nat Genet 43: 185-187.
23. Venables B, Ripley B (2002) Modern Applied Statistics with S: Springer.
24. K. Gjessing H (2013) Haplin: Software for genetic association analyses in case-parent triads, case-control data (or combined case-parent control-parent triads), with SNP haplotypes from candidate genes or GWAS data. 5.3 ed.
25. Team TRDC (2010) R: A Language and Environment for Statistical Computing. Version 2.11.1 ed: The R Foundation.
26. Sergeant J, Warwick J, Evans DG, Howell A, Berks M, et al. (2012) Volumetric and Area-Based Breast Density Measurement in the Predicting Risk of Cancer at Screening (PROCAS) Study. In: Maidment AA, Bakic P, Gavenonis S, editors. Breast Imaging: Springer Berlin Heidelberg. pp. 228-235.
27. Heine JJ, Cao K, Thomas JA (2010) Effective radiation attenuation calibration for breast density: compression thickness influences and correction. Biomed Eng Online 9: 73.
28. Ding J, Warren R, Warsi I, Day N, Thompson D, et al. (2008) Evaluating the effectiveness of using standard mammogram form to predict breast cancer risk: case-control study. Cancer Epidemiol Biomarkers Prev 17: 1074-1081.
29. Boyd NF, Martin LJ, Yaffe M, Minkin S (2009) Mammographic density. Breast Cancer Res 11 Suppl 3: S4.
30. Byrne C (1997) Studying mammographic density: implications for understanding breast cancer. J Natl Cancer Inst 89: 531-533.
31. Hofvind S, Geller B, Skaane P (2008) Mammographic features and histopathological findings of interval breast cancers. Acta Radiol 49: 975-981.
32. Ciatto S, Bernardi D, Calabrese M, Durando M, Gentilini MA, et al. (2012) A first evaluation of breast radiological density assessment by QUANTRA software as compared to visual classification. Breast 21: 503-506.
33. McEntee MF, Damases CN. Mammographic density measurement: a comparison of automated volumetric density measurement to BIRADS; 2014. pp. 90370T-90370T-90378.

34. Brand JS, Czene K, Shepherd JA, Leifland K, Heddson B, et al. (2014) Automated Measurement of Volumetric Mammographic Density: A Tool for Widespread Breast Cancer Risk Assessment. Cancer Epidemiol Biomarkers Prev.
35. Gonzalez RC, Woods RE (2008) Digital Image Processing: Pearson.
36. Belkhodja L, Benamrane N. Approche d'extraction de la région globale d'intérêt et suppression des artefacts radiopaques dans une image mammographique; 2009; Biskra, Algeria. *Symposium international: images, multimédias, applications, graphiques et environnements, IMAGE'2009*. pp. 239-248.
37. Pham DL, Xu C, Prince JL (2000) Current methods in medical image segmentation. Annu Rev Biomed Eng 2: 315-337.
38. Cheddad A, Mohamad D, Manaf AA (2008) Exploiting Voronoi diagram properties in face segmentation and feature extraction. Pattern Recognition 41: 3842-3859.
39. Costa L, Cesar R (2001) Shape Analysis and Classification: CRC Press.
40. Wirth MA, Stapinski A. Segmentation of the breast region in mammograms using active contours; 2003. *Proceedings of the SPIE visual communications and image processing*. pp. 1995-2006.
41. Ferrari RJ, Rangayyan RM, Desautels JE, Borges RA, Frère AF (2004) Identification of the breast boundary in mammograms using active contour models. Med Biol Eng Comput 42: 201-208.
42. Berks M (2010) Statistical models for synthesising the appearance of mammographic masses: University of Manchester.
43. Cheddad A, Svensson C, Sharpe J, Georgsson F, Ahlgren U (2012) Image processing assisted algorithms for optical projection tomography. IEEE Trans Med Imaging 31: 1-15.
44. Hörnblad A, Cheddad A, Ahlgren U (2011) An improved protocol for optical projection tomography imaging reveals lobular heterogeneities in pancreatic islet and β-cell mass distribution. Islets 3: 204-208.

Figure Legends

Figure. 1. (a) Scatter-plots of our PD measurements (processed mammograms) and Volpara (raw mammograms) measurements for the training sample of GE mammograms from 403 women (b) scatter-plots of our PD measurements and Volpara measurements for the test sample of GE mammograms from 1011 women with genotype information.

Figure. 2. -$\log_{10}$ QQ plots for p-values assessing the association between the investigated features (Table S1 and APs) and *rs10995190*. (a) with adjustment for age, BMI, menopausal status, HRT use, parity and age at first birth. (b) with adjustment as in *(a)*, plus Volpara. (c) with adjustment as in *(a)*, plus CASAM-Vol. (d) with adjustment as in *(a)*, plus CASAM-Area.

Tables

Table 1: Key characteristics of individuals included in this study (mean (s.d) or n (%)).

	Data used for developing CASAM-Vol (n = 403)	Data used for genetic association study (*) (n=1011)	Cases used for case-control study (n=47)	P-value (ψ) (comparing columns 3&4 data sets)
Age	55.93 (9.12)	53.52 (9.45)	58.59 (8.43)	< 0.001
BMI	25.12(4.17)	25.92 (4.46)	25.67 (4.27)	0.710
Postmenopausal				0.003
No	148 (37)	508 (50)	33 (69)	-
Yes	240 (60)	477 (47)	14 (29)	-
HRT use				0.041
Never	241 (60)	707 (70)	35 (73)	-
Past	102 (25)	204 (20)	6 (13)	-
Current	30 (7)	42 (4)	6 (13)	-
Parity and age at first birth				0.286
Nulliparous	49 (12)	101(10)	9 (19)	-
Parity ≤2 and age at first birth ≤25	95 (24)	250 (25)	13 (27)	-
Parity ≤2 and age at first birth >25	131(33)	380 (38)	16 (33)	-
Parity >2 and age at first birth ≤25	78 (19)	154 (15)	7 (15)	-
Parity >2 and age at first birth >25	35 (9)	99 (10)	2 (4)	-
Acquisition Parameters (APs)				
KVP	29.11 (1.17)	29.44 (1.07)	29.34 (1.13)	0.332
XTC	68.73 (14.75)	66.28 (12.40)	68.57 (14.76)	0.184
ExposureTime	721 (252.86)	819 (316)	767 (293)	0.230
XRayTubeCurrent	68.12 (14.66)	65.68 (12.39)	68.14 (14.82)	0.175
Exposure	47.42 (13.40)	52.59(18.03)	50.37 (15.89)	0.390
ExposureInMicroAs	47403 (13388)	52574 (18023)	50353(15844)	0.377
BodyPartThickness	58.53 (14.53)	61.43 (14.03)	59.02 (14.04)	0.232
AnodeTargetMaterial	0.823 (0.38)	0.884 (0.32)	0.823 (0.38)	0.195
RelativeXrayExposure	4748 (1746)	5426 (2280)	5116 (2025)	0.329
OrganDose	0.010 (0.0022)	0.011 (0.0031)	0.011 (0.0027)	0.277
CompressionForce	102 (29.69)	101 (30)	106 (27.99)	0.209
Volpara (raw)	2.01 (0.56)	2.01 (0.58)	2.12 (0.60)	0.159
CASAM-Area (Processed)	4.58 (1.02)	4.57 (1.03)	4.78 (1.01)	0.160
CASAM-Vol (Processed)	2.01 (0.49)	2.01 (0.50)	2.08 (0.51)	0.393

(*) Also used as controls in the case-control study. (**ψ**) Wald test p-values (logistic regression, unadjusted). (**) LR tests for menopausal status, HRT use and parity.

Table 2: Effect estimates for *rs10995190* on automated measures of mammographic density. Point estimates, interval estimates and p-values (Wald tests) are based on estimated coefficients for the SNP in linear regression models with PD measures as outcomes, adjusting for potential confounding variables (n=1011).

Outcome	Estimate (95%CI)	p-value
Volpara (raw)	-0.138 (-0.191,-0.085)	4×10^{-7}
CASAM-Area (Processed)	-0.254(-0.353,-0.155)	6×10^{-7}
CASAM-Vol (Processed)	-0.113(-0.158,-0.068)	9×10^{-7}

Table 3: p-values assessing the association of the automated measures of mammographic density with *rs10995190* (after additional adjustment for one other density measure) (n=1011).

Outcome variable	Variables adjusted for			
	Standard(*)	Standard+ Volpara	Standard+ CASAM-Area (Processed)	Standard+ CASAM-Vol
Volpara	4×10^{-7}	-	0.036	**0.079**
CASAM-Area (Processed)	6×10^{-7}	0.048	-	**0.147**
CASAM-Vol (Processed)	9×10^{-7}	**0.198**	**0.282**	-

(*) adjusting for age, BMI, menopausal status, HRT use, parity and age at first birth.

Table 4: Effect estimates for automated measures of mammographic density on case-control status, n=1058 (Cases 47, Controls 1011). Point estimates, interval estimates and p-values (Wald tests) are based on estimated coefficients for PD in logistic regression models with case-control status as outcome. (a) with partial adjustment (age and BMI), (b) with full adjustment (age, BMI, menopausal status, HRT use, parity and age at first birth).

Covariate	Estimate (95%CI)	p-value
(a)		
Volpara(raw)	0.978(0.300,1.660)	0.005
CASAM-Area (Processed)	0.483(0.112, 0.862)	0.012
CASAM-Vol (Processed)	0.926 (0.124,1.730)	0.023
(b)		
Volpara(raw)	0.961 (0.239, 1.706)	0.010
CASAM-Area (Processed)	0.467 (0.071, 0.879)	0.023
CASAM-Vol (Processed)	0.813 (-0.041, 1.691)	0.065

528 **Table 5:** p-values assessing the (residual) association between automated measures of mammographic density and
529 case-control status (after adjustment for one other density measure). (a) with partial adjustment (age and BMI), (b)
530 with full adjustment (age, BMI, menopausal status, HRT use, parity and age at first birth) (n=1058).

Covariates	**Variables adjusted for**			
(a)	Standard	Standard+ Volpara	Standard+ CASAM-Area (Processed)	Standard+ CASAM-Vol
Volpara	0.005	-	0.479	**0.823**
CASAM-Area (Processed)	0.012	0.162	-	**0.960**
CASAM-Vol (Processed)	0.023	**0.088**	**0.235**	-
(b)				
Volpara	0.010	-	0.529	**0.561**
CASAM-Area (Processed)	0.023	0.172	-	**0.769**
CASAM-Vol (Processed)	0.065	**0.054**	**0.158**	-

531

532

Response to Reviewer 1

We thank you for your helpful comments. We respond to each comment, in turn, below. Changes to the manuscript are highlighted in yellow.

Your comment 1:

The spelling should be check carefully, hundreds of misprints were full in the manuscript, such as VolparaTM (VolparaTM), and the space between the citation number with the sentence, such as "deletes it[9]", please check the manuscript again to avoid such mistakes.

Our response:

Volpara was referred to in the text as Volpara™ (TM as superscript in all instances). TM is a symbol that stands for a trademark and is conventionally used to denote commercial software.

In the revised manuscript we have changed Volpara™ to Volpara® (® denoting registered trademark). We use this symbol just once when we first introduce the software. In remaining instances we write Volpara without this symbol. We have also created a space between each citation number and its preceding sentence, based on your recommendation. Furthermore, we have carefully checked the manuscript for typographical and grammatical errors.

Your comment 2:

The coefficients of correlation of Figure 1 and Figure S2 were unknown, which should be provided in the result section. Additionally, the result and conclusion should be provided in detail for each figure and table. (Lines 234-241).

Our response:

We now include the appropriate correlation coefficients in Figure 1 (a & b) (Figure 1 and Figure S2 in the previous version) and in the text (lines: 240-241 and 245-246). Each Figure and Table is now properly discussed in the text (see, for example, p. 11).

Your comment 3:

The data and the codes should be provided as the supplementary, therefore, it can be repeated by other researchers. R packages would be preferred.

Our response:

We now make available (in supporting information files) all underlying measurements and data that have been used to derive the results in this study. Since we have carried out standard statistical analysis (linear and logistic regression) it is not appropriate to construct an R package. However, we do provide a file

which includes the R commands (along with the data set) that we used, so that it is possible for the reader to replicate our results.

Your comment 4:

As the authors said, CASAM-Vol appeared to mimic well Volpara and CASAM-Vol complement with CASAM-Area in some content. Therefore, why not design a statistic which can integrate both area and volume information simultaneously.

Our response:

Thank you very much for the hint. We now discuss this issue (Lines 283-287) and we refer to our previous publication which describes a simple approach for combining area and volumetric density (for analog images) (Ref. [14] in the manuscript).

Your comment 5:

the abbreviation "APs" in line 256 was unclear and never be reported in other part of the paper.

Our response:

Thank you again. This was a mistake on our part. The APs abbreviation stands for acquisition parameters and we now spell this out (page 3, line: 58).

Your comment 6:

A) in the line of 255, the author should provide the result which is similar with Figure 2b with the adjusted by CASAM-Vol and Volpara-Area.

B) in the line of 256, "After adjusting additionally for Volpara, there remained some evidence of association", this is the result. However, what's the conclusion? More analysis should be conducted to get the reason to interpret this result.

Our response:

A) We are not completely sure which variables you would like us to adjust for (there is no such measure *Volpara-area* in our manuscript). We expect however that you would like us to show the QQ plots summary associations adjusting for each of the two measures for processed images (CASAM-Vol and CASAM-Area); in turn. We now include these QQ plots. See Figure 2c (CASAM-Vol) & Figure 2d (CASAM-Area).

B) We refer to this finding in the discussion (Lines: 314-316):

> "It is possible that the density measures studied in the paper are unable to capture every aspect of density completely. This is supported, in our data, by the fact that the association between *rs10995190* and statistical/textural features does not completely disappear after adjusting for these PD measures."

It is difficult to interpret biologically the significance of individual features. For this reason we do not, for example, interpret biologically the feature with strongest evidence of association. We have expanded our discussion of this topic (see lines 316-321).

> "No single feature sticks out from the others in terms of its association with rs10995190 and furthermore it is difficult to interpret individual statistical/textural features in mammographic images [29-31].The features could relate directly to some biological change in breast composition but, on the other hand, these features could be capturing some aspect of the X-ray energy that is a proxy for breast composition or dense tissue thickness."

Your comment 7:

The manuscript should be re-arrange, numeric of important results were distributed in the supplementary section which caused the reading was confused, such as Figure S2. they should be merge together with other similar figure and be put in the main body.

Our response:

We have now moved Figure S2 and Table S3 into the main text. Figure S2 is now combined with Figure 1.

Response to Reviewer 2

Thank you for your insightful comments. We respond to each of them, in turn, below. All changes in the manuscript are highlighted in yellow.

Your comment 1:

The distribution of the final CASAM-Vol score is not well described. If the distribution is not normal, data should be transformed before analysis.

Our response:

CASAM-Vol inherits the normal distribution of *log* (Volpara) since it was trained against it. CASAM-Area is right-tailed which is why we used the square-root transformation to render the distribution normal. Area PD measures are typically transformed in the literature. Thus, all PD variables were transformed in such a way to make their distributions approximately normal, prior to analysis.

We state the following (Lines 197-199): "For CASAM-Area we used the square-root transformation, as in [2, 22], to obtain a variable which follows an approximate normal distribution. For Volpara measurements we used a logarithm transform since the distribution of the untransformed measurements are more heavily skewed than the area based measures."

Your comment 2:

The association tests shows PD measures by Volpara, CASAM-Area and CASAM-Vol are associated with rs10995190, and the association is weaken when adjusted for other measures. However, this is not necessary mean those measures are similar. Correlation, or the agreement between methods using BIRADS system, could be better indicator for the equivalences.

Our response:

The reason for carrying out these association tests, adjusting for other density measures, was to shed light on whether one measure picks up important aspects of density missed by others. We agree though that it is useful to provide more information about the correlation/agreement between the different density measures. The Pearson's correlation coefficients between CASAM-Area/CASAM-Vol and Volpara are now reported in the main text (Lines 240-241 for the training data set and lines 245-246 for the test data set). Although CASAM-Vol is meant to be highly correlated with Volpara (r=0.91), CASAM-Area's approach of measuring percent density is conceptually different to Volpara. The correlation between CASAM-Area and Volpara was, however, fairly strong (r=0.84). One of the main purposes of our work is indeed to contrast a projected-volume and a true volume (Lines 248-249).

Your comment 3:

Does the authors have PD% validated by radiologist? Although Volpara is a validated estimation of PD%, it is better to have the CASAM values compared with other subjective or semiautomated methods.

Our response:

The images included in this study have not been read by a subjective or semi-automatic method. We note, however, that the association between Volpara and Cumulus (the established percent density semi-automatic method) has previously been reported to be high (Ref. [13] in the manuscript) and that Volpara has also been shown to be strongly associated with MRI density measurements (r =0.93) (Ref. [9] in the manuscript). Quantra (an earlier version of Volpara) has also been shown to be associated with the BIRADS classification (89.0% correct classification) (Ciatto et al. 2012), and in another recent study Volpara density classification and radiologist's BIRADS showed a positive strong correlation ($r=0.87$; $p<0.001$) (McEntee et al. 2014). A discussion of these points is included in the manuscript (lines 353-360).

Ideally, it would be nice to have Cumulus measurements for the images included in this study but it is a tedious task considering the high volume of images that need to be processed (i.e., more than 1400 images) and moreover we do not have a trained Cumulus user.

Your comment 4:

In supplementary methods line 24, why do you down-sample the image to 512 pixels? Is it for saving the running time? What's the original size of the image? Also the bilinear resampling is not as good as other methods, I'm worried about the noise introduced by image down-sampling.

Our response:

To ease addressing this comment, we break it down into parts.

Why do we down-sample the image to 512 pixels? What's the original size of the image?

As you rightly speculate, the main sought advantage for down-sampling was to optimise the computational cost, because we need to process a large volume of images in one go. The elapsed time for pre-processing and calculating the set of features from one image (on average) was 19.3 seconds (resized image) and 13.7 min for a **full size image** (**5355×4915 pixels**). It is not uncommon to resize images in this way. There are many examples in the literature for mammographic images (Ferrari et al. 2004; Stylianos et al. 2011; Kallenberg and Karssemeijer, 2008; Penn et al. 2006; Luo et al. 2005; Ghouti L and Owaidh, 2014).

Also the bilinear resampling is not as good as other methods, I'm worried about the noise introduced by image down-sampling.

Noise could be an issue for screen-film mammography; however, the advantages of FFDM over screen-film mammography are numerous and they include wider latitude, lower noise and higher signal-to-noise ratio (PSNR); see Nishikawa (2003).

The above statement is also quantitatively endorsed by our calculations. As seen in the below table, the amount of noise present in the original FFDM image (and in its bilinear interpolated version) is very insignificant and unlikely to thwart our analysis.

Resizing method	Wiener noise power estimate	PSNR
Nearest-neighbor interpolation	7.4247e-04	44.1431
Bilinear interpolation	**6.9902e-04**	**46.0357**
Bicubic interpolation	7.4192e-04	44.4006
Box-shaped kernel	7.4247e-04	44.1431
Lanczos-2 kernel	7.4238e-04	44.3728
Lanczos-3 kernel	7.6103e-04	43.6003
Original Image	1.0622e-04	48.5053

The bilinear interpolation was coded in such a way as to preserve the aspect ratio and perform anti-aliasing. To contrast the performance of the different interpolation methods we used two metrics (shown in the table above) which are known to capture impulse noise power (the adaptive Wiener noise power estimator) and the signal-to-noise ratio (PSNR). The lower the noise-estimate the better and the higher the PSNR value the better. If we, for example, take the original image and add a Gaussian white noise of mean "0" and variance "0.01", the Wiener estimate becomes 0.0049 and the PSNR becomes 25.8117. As can be seen from the table, the differences in Wiener estimates from different interpolation methods are small/negligible. That said, the bilinear interpolation appears to perform the best.

Your comment 5:

Since the raw-to-processed conversion algorithm varies between manufactures, the author should discuss the generalizability of their methods on other Vendor machines.

Our response:

We have added the following text to our discussion (Lines 362-377).

"We expect that the PD measures for processed FFDM images, presented here, will perform consistently for mammograms taken from GE machines. There will, however, inevitably be some variability across different vendor machines due to discrepancies in raw-to-processed conversion algorithms. To address this issue, in cohorts comprising mammograms from different vendor machines, it may be necessary to retrain CASAM-Vol to mimic Volpara on each specific machine. Note that CASAM-Vol is constructed from features which include various acquisition parameters that are also exploited by Volpara and are X-ray system dependent (i.e., are not affected by the raw-to-processed conversion algorithm). We expect that CASAM-Vol can mimic Volpara with similar accuracy across different machines. Brand et al. [34] have

shown that there are only small differences in distributions of Volpara measurements across different vendor machines. It will therefore probably not be crucial (but it could still be wise) to adjust for machine in case/control or genetic association analyses based on CASAM-Vol. CASAM-Area is more likely, than CASAM-Vol, to be affected by raw-to-processed conversion variability. Like all threshold based methods in the literature, CASAM-Area is image intensity dependent. This intensity is greatly manipulated in an unpredictable way by the raw-to-processed conversion algorithms. For CASAM-Area it will be important to adjust for machines when fitting statistical models in studies incorporating multiple mammography machines."

Minor Comments:

1. There is no fitted line for CASAM-Area in figure 1 and figure s2.

We have now added this line to the plot; see Figure 1 (which now combines figure 1 and figure S2 in the previous version).

2. The correlation r is missing in Figure 1?

We have now calculated this and included it in the revised manuscript; see lines (240-241).

References:

Ciatto, S. et al. A first evaluation of breast radiological density assessment by QUANTRA software as compared to visual classification. The Breast, Volume 21, Issue 4, August 2012, Pages 503-506.

McEntee MF and Damases CN. Mammographic density measurement: a comparison of automated volumetric density measurement to BIRADS, Proc. SPIE 9037, Medical Imaging 2014: Image Perception, Observer Performance, and Technology Assessment, 90370T (March 11, 2014).

Ferrari RJ, Frère AF, Rangayyan RM, Desautels JEL, Borges RA. Identification of the breast boundary in mammograms using active contour models. Medical and Biological Engineering and Computing 2004, Volume 42, Issue 2, pp 201-208.

Stylianos D. Tzikopoulos, Michael E. Mavroforakis, Harris V. Georgiou, Nikos Dimitropoulos, Sergios Theodoridis, A fully automated scheme for mammographic segmentation and classification based on breast density and asymmetry, Computer Methods and Programs in Biomedicine, Volume 102, Issue 1, April 2011, Pages 47-63, ISSN 0169-2607,

Penn A, Thompson S, Brem R, Lehman C, Weatherall P, Schnall M, Newstead G, Conant E, Ascher S, Morris E, Pisano E, Morphologic Blooming in Breast MRI as a Characterization of Margin for Discriminating Benign from Malignant Lesions, Academic Radiology, Volume 13, Issue 11, November 2006, Pages 1344-1354,

Luo P, Qian W, Romilly P, CAD-Aided Mammogram Training1, Academic Radiology, Volume 12, Issue 8, August 2005, Pages 1039-1048.

Kallenberg M and Karssemeijer N. Computer-aided detection of masses in full-field digital mammography using screen-film mammograms for training. 2008 Phys. Med. Biol. 53 6879.

Ghouti L and Owaidh A.H. NMF-Density: NMF-Based Breast Density Classifier. ESANN 2014 proceedings, European Symposium on Artificial Neural Networks, Computational Intelligence and Machine Learning. Bruges (Belgium), 23-25 April 2014, pp: 445-460.

Nishikawa R.M. 2003. Computer-aided detection in digital mammography. In: E.D. Pisano, M.J. Yaffe and C.M.Kuzmiak (Eds.). Digital mammography. USA: Lippincott Williams & Wilkins, pp: 43-48.